MICROSCOPIC CALCULATION OF DEFORMATION ENERGIES OF NUCLEI

By

ANUP KUMAR DUTTA, M.Sc.

A Thesis

Submitted to the School of Graduate Studies

in Partial Fulfilment of the Requirements

for the Degree

Doctor of Philosophy

McMaster University

September 1980

To my Parents

DOCTOR OF PHILOSPHY (1980)
(Physics)

McMASTER UNIVERSITY
Hamilton, Ontario

TITLE: Microscopic calculation of deformation energies of nuclei

AUTHOR: Anup Kumar Dutta, M.Sc. (Ravishankar University)
M.Sc. (McMaster University)

SUPERVISOR: Professor R. K. Bhaduri

NUMBER OF PAGES: vii, 90

ABSTRACT

For a given two-body force, we formulate a method for estimating the energy in a constrained Hartree-Fock calculation of a deformed nucleus. This is done by using the information from the first two iterations of the self-consistency cycle. After giving some simple illustrations, the method is applied to obtain the deformation energy curve of some medium heavy nuclei and the fission barrier of ^{240}Pu. The results are compared with the corresponding self-consistent CHF calculations with a standard Vautherin-Brink type Skyrme force to ascertain the accuracy of the method. We investigate further the density dependence of the fission barrier of ^{240}Pu by using five different Skyrme-type forces. The barrier height systematic in relation to the incompressibility and surface energy is investigated. The Kyoto S-MK interaction gives the best results. The energy surfaces of ^{232}Th, ^{252}Fm and ^{258}Fm are also traced with this force. It is found that the Thorium-anomaly persists in our microscopic calculation. Consistent with the usual interpretation of the experimental data, we find a vanishing second barrier for ^{258}Fm.

ACKNOWLEDGEMENTS

It is a great pleasure to thank my supervisor Prof. R. K. Bhaduri for suggesting the problem and for his guidance and encouragement throughout the work of my thesis.

I would also like to thank the members of my supervisory committee, Profs. Y. Nogami, P. Yip and R. Kelly for their interest and support.

Throughout the course of this work I have benefitted from the suggestions of people in and out of the theory group, and I gratefully acknowledge their help. Especially I would like to mention Drs. M. Vallières, I. Easson and M. K. Srivastava for collaboration in the early stages of this work and Dr. M. Kohno for collaboration in later stages. Prof. M. Brack's help in pointing out the technical difficulties met in fission barrier calculations has been invaluable. Prof. D.W.L. Sprung has always made himself available for looking into my computational problems.

During my stay at McMaster I have made many friends who have made my stay enjoyable and memorable. To them all I thank profusely. In particular I would like to mention Aamir, Kalpana, Narendra, Raj, Rasheeda, Sudesh and Tariq whose friendship and warm affection has always made me feel at home. Mention must also be made of the supper club members, King Eff, Sir Azob, Sir Maharg and Z.

A special word of thanks goes to Mrs. Helen Kennelly for her careful and paitent job of typing this thesis, and for bringing in the morning newspaper every day.

Finally I would like to thank McMaster University for financial assistance in the form of a teaching assistantship.

TABLE OF CONTENTS

CHAPTER I

INTRODUCTION

I.1 Historical Introduction

The theory of nuclei is to be contrasted with the theory of atoms. Whereas the nature of force between the constituent particles in an atom is well known, the same is not true for the nucleons in a nucleus. Therefore, in the nuclear case, nucleon-nucleon (N-N) scattering data are examined to fit the parameters of a model potential. Many body calculations of static nuclear properties with these realistic potentials have been attempted[1)] in the framework of Goldstone expansion. The results are found not very satisfactory either due to the inadequacy inherent in the potential used or due to inclusion of only a limited class of terms in the perturbative series. These complications have encouraged the use of effective interactions. This has been possible because the short range attractive N-N interaction which becomes repulsive at even smaller distances can be replaced by an effective interaction. The Pauli principle prevents the nucleons from coming too close to each other, thereby suppressing the repulsive part of the N-N interaction. There are two ways to derive the effective forces. In the first, it is derived in the lowest

order from a realistic two nucleon interaction. In Brueckner's theory this is the G-matrix. Certain higher order terms are then added[2,3] which are parametrized. The second method is based on the philosophy that since the macroscopic properties of nuclei are not expected to depend extensively on tne detailed structure of the interaction, one may achieve some success by adopting some averaged and simplified version. Thus no help is taken from the realistic N-N interaction and the effective force is completely parametrized. The parameters may be fitted from the saturation properties of nuclear matter and the properties of spherical nuclei. Although this procedure is less fundamental than the first method, it is widely used since the calculations are much simpler and better physical insight can be obtained since relations between various physical quantities turn out to be quite simple. Further, one can extrapolate quite confidently to study the nuclides in superheavy region and the nuclei away from the stability line.

The effective forces that are used for present day calculations are density dependent. The idea stems from the fact that a purely attractive force is unable to produce saturation in nuclear matter and that the nuclear force must have other characteristics too to prevent any collapse. One of these is the tensor force which does not contribute to the binding energy in first order but contributes in second order.

This contribution increases with increasing density and flattens out at nuclear matter density. Also, at high densities, a short range repulsive part will prohibit further collapse. Further, the contribution from exchange character of nuclear force depends on the density of the system. Examples of interactions which are density dependent are the Moszkowski's δ-interaction[4] and the Skyrme interaction[5]. A simple version of the latter, developed by Vautherin and Brink has been implemented in Hartree-Fock calculations of spherical[6] and deformed[7,8,9] nuclei with much success and has become popular in recent years. Negele and Vautherin[10] have shown that starting from the reaction matrix derived from the nuclear matter theory in the local density approximation one can obtain a density dependent interaction. Further, if the density matrix is expanded in relative and centre-of-mass coordinates and all derivatives beyond second order are neglected, then one obtains an expression for energy density very similar to that of Skyrme interaction. This gives some justification for the use of Skyrme interactions. The advantage of calculation with Skyrme forces performed in the Hartree-Fock approximation is that the resulting energy density is local and the numerical solutions are obtained much faster than the corresponding solutions with finite range interactions. The use of Hartree-Fock approximation is justified to some extent by the success of phenomenological shell model.

Once the ground state properties of nuclei have been studied with Skyrme interaction, it is interesting to see how well the nucleus is described away from its ground state. Such a situation, for example, occurs in the fission process. Experimental estimates of the barrier heights are available for comparison. Very few microscopic calculations for fission have been attempted[11,12,13]. Those with Skyrme interaction have been performed with the constrained Hartree-Fock technique[9]. It is not clear from these calculations if the experimental barrier heights are reproduced, because many degrees of freedom through which fission can take place are not explicitly included in the calculations. Therefore, at best one can make a rough estimate for the contribution from these degrees of freedom. Further, the barrier heights seem to be quite sensitive to pairing which is added in the BCS approximation to the Hartree-Fock results. It might be therefore interesting to attempt to study the systematic variation of barrier height with various Skyrme forces or with their modified versions. However, such a project is too time consuming and expensive computationally.

Several attempts have been made to find a substitute for the self-consistent method. The most notable among these is the Strutinsky shell correction method[14,15]. The macroscopic part of the binding energy which is supposed to be smoothly varying is taken from the phenomenological liquid-drop

formula. The fluctuating part of the binding energy which arises due to the shell effects is added as a correction to the liquid-drop part. This technique is much less time consuming and has been very successful in reproducing nuclear properties, especially the double hump fission barrier of actinides. However, one would still like to perform microscopic calculations, thereby having the advantage of simultaneously obtaining the smoothly varying properties as well as the single particle spectra which contributes to the fluctuating part. This excludes any inconsistency that might result from a dual approach in the shell correction method.

I.2 Scope of the Thesis

We realize that the Hartree-Fock calculations are very time consuming but are still desirable for reasons mentioned earlier. We have therefore attempted to find a simple approximation to the Hartree-Fock method. The approximation is microscopic although not variational. In sec. II.1 of Chapter II the main ideas about our method are laid down. A brief introduction to the Skyrme-type interactions appears in sec. II.2. As an interesting case, estimate of ground state energy of the helium atom where Coulomb interaction is the two-body force, is made in sec. II.3a. The binding energies of some spherical nuclei have been calculated with Skyrme III interaction in sec. II.3b.

For deformed nuclei, the constrained Hartree-Fock technique has been generally used for tracing energy versus deformation energy curves. Our method has been modified accordingly in sec. III.1. In sec. III.2 we discuss the various degrees of freedom that have been allowed in our deformed starting Woods-Saxon field. Corrections due to pairing, which is important in deformed nuclei, are discussed in sec. III.3. Some technical details about the choice of basis states onto which the Hartree-Fock wave functions are projected, are given in sec. III.4. Finally, in sec. III.5 two deformed nuclei, ^{134}Ce and ^{168}Yb, have been taken as examples and results of our approximation are compared with the corresponding self-consistent results.

In Chapter IV we have looked into the fission barrier of ^{240}Pu. After a brief discussion on the phenomenon of fission in general in sec. IV.1 and on the experimental methods to determine the barrier heights in sec. IV.2, we compare in sec. IV.3 the energy versus deformation curve with our method and with the Hartree-Fock method. To make comparison with the experimental barrier heights, certain corrections have to be made in our calculation which have been discussed in sec. IV.4. The Vautherin-Brink version of Skyrme force has been shown to be incapable of producing the correct barrier heights. Therefore some other Skyrme-type interactions have been looked into in sec. IV.5, which have very different bulk

properties in nuclei. These interactions have been employed to trace the potential energy surface of ^{240}Pu using our approximation in sec. IV.6. The interaction which yields barrier heights in rough agreement with the experimental estimates is chosen for the latter calculations. In sec. IV.7 fission barriers of some other actinides are calculated using our method. In sec. IV.7a, ^{232}Th has been considered. It has been shown that the "Thorium anomaly" exists in our microscopic calculation also. In sec. IV.7b, barriers of two isotopes of Fermium, ^{252}Fm and ^{258}Fm have been calculated. The disappearance of second barrier in ^{258}Fm has been shown here which is in accordance with the results of some microscopic-macroscopic calculations.

In summary, we have proposed an approximate microscopic method which has been used to obtain the ground state energies of nuclei and to study their fission barrier systematics. Attempt has been made to find some correlation between the bulk properties of a nucleus calculated from effective one-body fields and the corresponding barrier heights.

CHAPTER II

THE APPROXIMATION

As yet, an exact treatment of the nuclear many-body problem has not been possible. Some approximations are therefore necessary. In view of the success of the independent particle (Hartree-Fock) approximation in atomic physics, one is tempted to apply the technique to a nuclear system. Although the characteristics of the nuclear force are quite different from the coulomb force, the validity of the idea that the nucleons move quite independently of each other in a mean field in the nucleus is borne out by the success of the shell-model. Because of the Pauli exclusion principle, which prohibits scattering into already occupied states, the nucleonic mean free path is much larger than the characteristic internucleonic distance. Some idea about the mean free path in a nucleus can be obtained from the ratio of the volume of the nucleus to the elastic scattering cross-section which turns out to be much larger than the internucleonic distance.

The static Hartree-Fock (HF) approximation consists of searching for a Slater determinant which will yield a minimum for the expectation value of the effective Hamiltonian of the system. The advantage of such a calculation is that one is able to describe simultaneously such different quantities as binding energy, charge radius, quadrupole moment etc. of a

nucleus, whereas different phenomenological approaches may be needed to describe each of these quantities. The HF calculations for spherical nuclei are fast and efficient, but deformed nuclear calculations are very time consuming to compute. In spherical nuclei, one seeks for convergence in total energy of the system, whereas in deformed nuclei one demands self-consistency in the total energy as well as in a quantity like the quadrupole moment which is a measure of deformation which requires a large number of iterations. It is therefore important to devise alternate schemes for calculating the bulk properties of nuclei which are faster to implement. In this vein, semiclassical Thomas-Fermi type calculations[16,17] in spherical nuclei, and self-consistent WKB calculations[18] are worth mentioning. We have devised a method which is an approximation to the HF equation and uses only two iterations of the self-consistency cycle. The method which we shall call the "Two-step iterative method" (TSIM) is outlined in sec. II.1. A brief discussion of Skyrme-type forces has been given in sec. II.2 since they have been used here for all the nuclear calculations. Since any method proposed should be first tested in simple systems, we have applied the method to helium atom in sec. II.3a. Spherical nuclei have been considered in sec. II.3b and the binding energy estimates from the TSIM are compared with the corresponding HF estimates.

II.1 The two-step iterative method

Consider a many-fermion system which is adequately described by a Hartree-Fock scheme. Let the fermions interact with a two-body interaction which may or may not be density dependent. Then the HF energy for a system of N fermions of one kind in terms of the reduced density matrix of the ith particle, ρ_i is

$$E(\rho) = tr_1 \hat{t}_1 \rho_1 + \frac{1}{2} tr_1 tr_2 \rho_1 \rho_2 v_{12} , \qquad (2.1)$$

where the first term on the right hand side denotes the kinetic energy

$$- \frac{\hbar^2}{2m} \int d\underset{\sim}{r}_1 \nabla^2_{r_1} \rho(\underset{\sim}{r}_1, \underset{\sim}{r}_1') \Big|_{\underset{\sim}{r}_1 = \underset{\sim}{r}_1'} ,$$

and ρ_i is normalised such that $tr_i \rho_i = N$. The self-consistent one body field is $\hat{U}_1 = tr_2 \rho_2 v_{12}$. The self-consistency cycle in the HF scheme is started with the choice of an appropriate trial single particle density $\rho_i^{(0)}$ such that $\delta\rho_i = \rho_i - \rho_i^{(0)}$. One can then write eqn. (2.1) as

$$E(\rho) = E^{(0)} + tr_1 (\hat{t}_1 + U_1^{(0)}) \delta\rho_1 + \frac{1}{2} tr_1 tr_2 \delta\rho_1 \delta\rho_2 v_{12} , \qquad (2.2)$$

where $E^{(0)} = E(\rho^{(0)})$ and $U_1^{(0)} = tr_2 \rho_2^{(0)} v_{12}$. Here the parenthesised superscript (0) denotes the "zeroth" iteration. We denote by $\rho_1^{(1)}$ the density generated after first iteration by solving in the one-body field $U^{(0)}$. Eqn. (2.2) can be rewritten as

$$E(\rho) = E^{(0)} + tr_1(\hat{t}_1+U_1^{(0)})(\rho_1^{(1)}-\rho_1^{(0)}) + tr_1(\hat{t}_1+U_1^{(0)})(\rho_1-\rho_1^{(1)}) + \frac{1}{2} tr_1 tr_2 \delta\rho_1 \delta\rho_2 v_{12} . \quad (2.3)$$

Now we make an approximation to eqn. (2.3) by dropping the last two terms. Our estimate for the HF energy is then

$$E(\rho) = E^{(0)} + tr_1(\hat{t}_1+U_1^{(0)})(\rho_1^{(1)}-\rho_1^{(0)}) . \quad (2.4)$$

In practice, one needs to compute $E^{(0)}$ from a suitable trial density $\rho^{(0)}$ and define through it the one-body field $U^{(0)}$. One then solves the HF equation in the field $U^{(0)}$ to obtain $\rho_1^{(1)}$ which satisfies

$$tr_1(\hat{t}_1+U_1^{(0)})\rho_1^{(1)} = \sum_{i_{occ}} \varepsilon_i^{(1)} , \quad (2.5)$$

where the right hand side term is the sum of single particle energies over the occupied states. Explicit computation of the integral $tr_1(\hat{t}_1+U_1^{(0)})\rho_1^{(0)}$ suffices for the approximate evaluation of $E(\rho)$. It should be noted that the inclusion of three-body forces does not change the final form of our approximation, although the one-body field $U^{(0)}$ is modified.

Although we cannot rigorously justify our approximation, we can take a look at the terms that have been neglected. The term $tr_1(\hat{t}_1+U_1^{(0)})(\rho_1-\rho_1^{(1)})$ can be written as

$$\sum_{i_{occ}} \varepsilon_i - \sum_{i_{occ}} \varepsilon_i^{(1)} - tr_1\rho_1\delta U_1 , \quad (2.6)$$

where the first term is the sum of HF single particle energies and $\delta U = U - U^{(0)}$, U being the self-consistent field. If $\rho_i^{(1)}$ is the particle density for the ith state obtained from solving in the field $U^{(0)}$, then by perturbation theory

$$\varepsilon_i^{HF} = \varepsilon_i^{(1)} + \int \delta U \, \rho_i^{(1)} d\underset{\sim}{r} \, , \tag{2.7}$$

to first order.

Also the other neglected term in eq. (2.3) $\frac{1}{2} \, tr_1 tr_2 \delta\rho_1 \delta\rho_2 v_{12}$ can be put in the form

$$\frac{1}{2} \, tr_1 \, \delta U_1 (\rho_1 - \rho_1^{(0)}) \, . \tag{2.8}$$

Thus the sum of the two neglected terms in eqn. (2.3) is then given by

$$tr_1 \, \delta U (\rho_1^{(1)} - \frac{\rho_1 + \rho_1^{(0)}}{2}) \, ,$$

which can be small.

It should be noted that although the correction term in eqn. (2.4) is reminiscent of the Strutinsky theorem[14], the connection between the two is remote. Our zeroth order estimate $E^{(0)}$ already contains shell effects, and no "smoothing" of any kind is involved.

II.2 Skyrme-type interaction

Since Skyrme-type interactions[19] have been used in all our calculations, a brief discussion of these is warranted. These interactions consist of a two body potential v_{12} of zero range and quadratic momentum-dependent terms. In addition to this, v_{12} contains a density dependent term. The two body spin-orbit interaction is used within the zero range approximation. So the most general parametrization of the Skyrme-type interaction is

$$\begin{aligned} v_{12} &= t_0(1+x_0P_\sigma)\delta(\underset{\sim}{r}_{12}) \\ &+ \tfrac{1}{2}\, t_1(1+x_1P_\sigma)(k'^2\delta(\underset{\sim}{r}_{12})+\delta(\underset{\sim}{r}_{12})k^2) \\ &+ t_2(1+x_2P_\sigma)\underset{\sim}{k}'\cdot\delta(\underset{\sim}{r}_{12})\underset{\sim}{k} \\ &+ \tfrac{1}{6}\, t_3(1+X_3P_\sigma)\rho^\beta(\underset{\sim}{R}_{12})\delta(\underset{\sim}{r}_{12}) \\ &+ iW(\underset{\sim}{\sigma}_1+\underset{\sim}{\sigma}_2)\cdot(\underset{\sim}{k}'\times\delta(\underset{\sim}{r}_{12})\underset{\sim}{k}) \ , \end{aligned} \tag{2.9}$$

where $\underset{\sim}{r}_{12} = \underset{\sim}{r}_1-\underset{\sim}{r}_2$, $\underset{\sim}{R}_{12} = (\underset{\sim}{r}_1+\underset{\sim}{r}_2)/2$, $\underset{\sim}{k} = (\overrightarrow{\nabla}_1-\overrightarrow{\nabla}_2)/2i$ and $\underset{\sim}{k}' = (\overleftarrow{\nabla}_1-\overleftarrow{\nabla}_2)/(-2i)$. W is the strength of the spin-orbit force.

One can recall the qualitative effects of the parameters in v_{12}. The parameters t_0 and t_1 correspond to interaction in the relative s- and d-states whereas t_2 governs the interaction in the relative p-state. The operator $P_\sigma\delta$ acting on the anti-symmetrized states is equivalent to $-P_\tau\delta$ where P_τ is the isotopic exchange operator. Therefore the coefficients x_0, x_1, x_2 and

x_3 determine to some extent the effect of neutron-proton asymmetry in the system. The parameter t_3 governs the extent to which the interaction between two nucleons is affected by the presence of others.

The main advantage of Skyrme-type interaction is that the energy density $H(\underset{\sim}{r})$ can be expressed locally in terms of the one-body diagonal density matrix $\rho(\underset{\sim}{r})$, the kinetic energy density $\tau(\underset{\sim}{r})$ and the spin density $\vec{J}(\underset{\sim}{r})$. For an A nucleon system

$$\rho(\underset{\sim}{r}) = \sum_{i=1}^{A} |\phi_i(\underset{\sim}{r})|^2$$

$$\tau(\underset{\sim}{r}) = \sum_{i=1}^{A} |\nabla\phi_i(r)|^2$$

and

$$\underset{\sim}{J}(\underset{\sim}{r}) = -i \sum_{i=1}^{A} \phi_i^*(\underset{\sim}{r}) \cdot (\nabla\phi(\underset{\sim}{r}) \times \underset{\sim}{\sigma}) \quad , \tag{2.10}$$

where $\phi_i(\underset{\sim}{r})$ are single particle HF wave functions. The nuclear part of the HF energy is then

$$E = \int d\underset{\sim}{r}\, H(\rho, \tau, \underset{\sim}{J}) \quad .$$

In addition, the repulsion between the protons should contribute to the total energy. The direct part of the Coulomb energy is local, but the exchange part is not. To keep matters simple, the exchange energy E_{exch} is made local, generally in the Slater approximation

$$E_{exch} = -\frac{3}{4} e^2 \left(\frac{3}{\pi}\right)^{1/3} \int \rho_p^{4/3}(\underset{\sim}{r}) d\underset{\sim}{r} , \qquad (2.11)$$

where $\rho_p(\underset{\sim}{r})$ is the proton density around $\underset{\sim}{r}$.

The parameters in the interaction v_{12} are obtained by fitting the saturation properties of magic nuclei because the calculations are simple due to spherical symmetry. The spin-orbit strength W is adjusted by fitting spin-orbit splitting energy of some magic nucleus or by adjusting as best as possible single-particle level ordering. The choice of a set of parameters is not unique. Beiner et al.[19] have shown that in the Vautherin-Brink version[6] of the Skyrme force where $x_1 = x_2 = 0$ and $x_3 = \beta = 1$, there is an infinite choice of parameter sets.

II.3 Simple applications

To check the accuracy of our method we test it on helium atom where the force is of long-range character and on some spherical nuclei using Skyrme III[20] force which has the short-range behaviour. We find that the approximation yields a very close estimate to the HF energy. It is also shown that as long as the trial density is at all reasonable, the final value of energy is fairly independent of the choice of trial density.

II.3a The Helium atom

The Hamiltonian of the two-electron system, taking the nucleus to be infinitely heavy at the origin is

$$\hat{H} = \frac{p_1^2}{2m} + \frac{p_2^2}{2m} - \frac{2e^2}{r_1} - \frac{2e^2}{r_2} + \frac{e^2}{|\underset{\sim}{r}_1 - \underset{\sim}{r}_2|}$$

$$= \hat{t}_1 + \hat{t}_2 + V_N(1) + V_N(2) + V_{12} .$$

Normalising the electron density ρ_i to unity in this case, one can write the HF energy as

$$E(\rho) = tr_1(\hat{t}_1+V_N(1))\rho_1 + tr_2(\hat{t}_2+V_N(2))\rho_2 + tr_1 tr_2 \rho_1 \rho_2 V_{12} .$$

The HF field is $U_1 = V_N(1) + tr_2\rho_2 V_{12}$. In the notation of section II.2, our estimate for the energy can be written as

$$E(\rho) = E^{(0)} + 2tr_1(\hat{t}_1+U_1^{(0)})(\rho_1^{(1)}-\rho_1^{(0)}) , \qquad (2.12)$$

where the extra factor 2 appears due to different normalization.

We choose the trial density $\rho^{(0)}$ in two different ways. First we use hydrogenic wave functions. The trial density is $\rho^{(0)} = \frac{1}{\pi}(2/a_0)^3 \exp(-4r_1/a_0)$ where the Bohr radius $a_0 = \hbar^2/me^2$. Then

$$E^{(0)} = E(\rho^{(0)}) = \frac{11}{2} E_H = -74.72 \text{ eV} ,$$

where E_H is the hydrogen atom ground state energy. Also the term $2tr_1(\hat{t}_1+U_1^{(0)})\rho_1^{(0)} = 3E_H = -40.76$ eV. Numerical computation yields

$$2tr_1(\hat{t}_1+U_1^{(0)})\rho_1^{(1)} = -44.60 \text{ eV}.$$

Thus eqn. (2.12) gives the estimate for total energy as $(-74.72 - 44.60 + 40.76) = -78.56$ eV as compared to the HF energy of -77.86 eV.

The second choice of $\rho^{(0)}$ is obtained from gaussian wave functions. Then

$$\rho^{(0)} = (\pi\alpha^2)^{-3/2} \exp(-r_1^2/\alpha^2) ,$$

which yields

$$E^{(0)} = \frac{\hbar^2}{2m}\frac{3}{\alpha^2} - \frac{8e^2}{\sqrt{\pi}\,\alpha} + \sqrt{\frac{2}{\pi}}\frac{e^2}{\alpha} .$$

The value of $\alpha = 0.427$ Å minimizes $E^{(0)}$ to give -62.52 eV. One can see that $\rho^{(0)}$ defined through the gaussian wave functions is certainly worse than that defined through hydrogenic functions. However, the correction term $\Delta E^{(1)} = tr_1(\hat{t}_1+U_1^{(0)})(\rho_1^{(1)}-\rho_1^{(0)})$ for the gaussian case is very different. One gets

$$2tr_1(\hat{t}_1+U_1^{(0)})\rho_1^{(0)} = -35.67 \text{ eV}$$

and

$$2tr_1(\hat{t}_1+U_1^{(0)})\rho_1^{(1)} = -51.51 \text{ eV} .$$

Thus the estimate for total energy in this case is $(-62.52 - 51.51 + 35.67) = 78.36$ eV which is remarkably close to the earlier result.

II.3b Spherical nuclei

We calculate the binding energies of the spherical nuclei ^{16}O, ^{40}Ca, ^{48}Ca, ^{90}Zr and ^{208}Pb using the Skyrme III force. The usual zero-range spin orbit force and the Coulomb force are included, but not the exchange contribution due to the latter force. We choose $\rho^{(0)}$ in two different ways. In the first case, spherical harmonic oscillator wave functions are chosen to define $\rho^{(0)}$. The oscillator constants for neutrons and protons are varied separately to minimize the energy $\int H(\underset{\sim}{r})d\underset{\sim}{r}$. This is simple to do because $\rho^{(0)}$ is analytically expressed in terms of the harmonic oscillator wave functions. The variational estimate of the energy is $E^{(0)}$. In performing the variation for $E^{(0)}$, the s-wave oscillator parameters for protons and neutrons are kept fixed by demanding the central density (at $r = 0$) to be $0.075\ fm^{-3}$ and $0.085\ fm^{-3}$ respectively. The final results are not very sensitive to these specific values so long as the central density is close to the nuclear matter value. For doubly closed nuclei ^{16}O, ^{40}Ca and ^{208}Pb, a two parameter variational calculation is performed to obtain $E^{(0)}$ and $\rho^{(0)}(\underset{\sim}{r})$, the variational parameters being one oscillator constant for protons in p,d,f,g$\cdots$ shells and likewise another constant for neutrons. It is found that for ^{48}Ca and ^{90}Zr, the final result for the energy improved by 2 or 3 MeV when the oscillator parameter of the last filled $f_{7/2}$-shell is taken to be an additional variational parameter. Otherwise, the final result does not

change (within an MeV or so) on increasing the number of variational parameters. It should be noted that $\rho^{(0)}$ is generated by potentials without spin-orbit force and weights all orbitals in the f-shell in ^{48}Ca and ^{90}Zr equally. Consequently, the spin-orbit component present in the one body field $U^{(0)}$ does not contribute to the last term of eqn. (2.4).

Another choice of $\rho^{(0)}$ is through Woods-Saxon wave functions. In this case, one loses the analyticity of $\rho^{(0)}$ but the accuracy of $E^{(0)}$ is much improved. Moreover, most standard HF codes have the option to start the iteration from a Woods-Saxon potential. This makes it easy to adapt the code to implement the TSIM. The choice of parameters for the potential are not crucial. We choose the standard values: depths of 44 and 40 MeV for neutron and proton wells with equal radii $1.27\ A^{1/3}$ and a diffuseness parameter of 0.67 fm. The effective mass is taken to be unity.

The results for the above-mentioned choices of $\rho^{(0)}$, are displayed in Table 1 and compared with the HF results. The parenthesized numbers correspond to the harmonic oscillator $\rho^{(0)}$. As in the case of helium atom, one can see here that the poorer choice of harmonic oscillator $\rho^{(0)}$ than the Woods-Saxon $\rho^{(0)}$ leads to a less accurate $E^{(0)}$ but to a correspondingly larger correction term $\Delta E^{(1)}$. However, as can be seen in Table 1, the final estimate of total energy is close to the HF value and is independent of the choice of $\rho^{(0)}$. It should be noted that the TSIM estimate can overshoot the HF energy since the

TABLE 1

THE TSIM ESTIMATES OF ENERGIES AND R.M.S. RADII OF CLOSED SHELL NUCLEI

Nucleus	$E^{(0)}$	$\Delta E^{(1)}$	$E^{(0)}+\Delta E^{(1)}$	E(HF)	$\langle r^2\rangle^{\frac{1}{2}}$ (1st iteration)		$\langle r^2\rangle^{\frac{1}{2}}$ (HF)	
					n	p	n	p
^{16}O	-106.52	-4.49	-111.01	-110.28	2.69	2.69	2.65	2.68
	(-106.28)	(-6.28)	(-112.56)		(2.70)	(2.73)		
^{40}Ca	-310.85	-8.67	-319.52	-318.06	3.42	3.44	3.38	3.43
	(-304.17)	(-14.72)	(-318.89)		(3.41)	(3.46)		
^{48}Ca	-383.75	-10.90	-394.65	-393.31	3.63	3.51	3.62	3.48
	(-346.45)	(-42.58)	(-389.03)		(3.67)	(3.54)		
^{90}Zr	-734.58	-17.75	-752.33	-749.74	4.33	4.34	4.32	4.27
	(-676.12)	(-75.54)	(-751.66)		(4.38)	(4.36)		
^{208}Pb	-1558.02	-30.82	-1588.84	-1587.44	5.69	5.60	5.66	5.53
	(-1373.48)	(-213.10)	(-1586.58)		(5.77)	(5.66)		

Energies and R.M.S. radii of closed shell nuclei. Energies are in MeV and radii are in fm. The numbers in brackets are the results with harmonic oscillator $\rho^{(0)}$. The unbracketed numbers are obtained by using $\rho^{(0)}$ obtained from a Woods-Saxon potential (parameters given in the text). The Sky III interaction has been used for the calculations. Coulomb exchange energy and the centre of mass motion correction are not included.

method is not variational. The correction factor $\Delta E^{(1)}$ in the harmonic oscillator $\rho^{(0)}$ can be 10% or more of the total energy. It is therefore unlikely, in ^{208}Pb for example, that the two neglected terms in eqn.(2.3) are individually small. Numerically, each of these terms is found to be of the order of 90 MeV in ^{208}Pb, but of opposite sign. That the terms are of opposite sign can be seen from the fact that for an attractive short-range force v_{12} the term $\frac{1}{2}\,tr_1 tr_2 \delta\rho_1 \delta\rho_2 v_{12}$ is always negative. On the other hand, since $\rho_1^{(1)}$ is generated by solving the Schrödinger equation in the one-body field $U_1^{(0)}$, the term $tr_1(\hat{t}_1+\hat{U}_1^{(0)})(\rho_1-\rho_1^{(1)})$ is always positive. The neglected terms for the Woods-Saxon $\rho^{(0)}$ are of the order of 5 MeV individually. For this reason and the fact that it is generally the starting field in HF codes, we have used the Woods-Saxon field in all our calculations in deformed nuclei.

In Fig. 1 the density $\rho_1^{(1)}$ for protons and neutrons is compared with the corresponding HF densities for ^{208}Pb. The agreement is not good in the interior. The surface and the tail are in somewhat better agreement. The situation is similar for the other nuclei considered. However, the point to be emphasized here is that a very accurate estimate of the energy of the system can be made by the TSIM without a detailed knowledge of the density profile. From Table 1, one can also see that the rms radii obtained through $\rho_1^{(1)}$ are within a percent or two of the HF values.

Fig. 1 Neutron and proton density distribution in ^{208}Pb. A comparison is made between $\rho^{(1)}$, the density after first iterations, and the self-consistent HF density ρ. The density $\rho^{(1)}$ has been generated by solving in the one-body field $U^{(0)}$ generated with harmonic oscillator $\rho^{(0)}$.

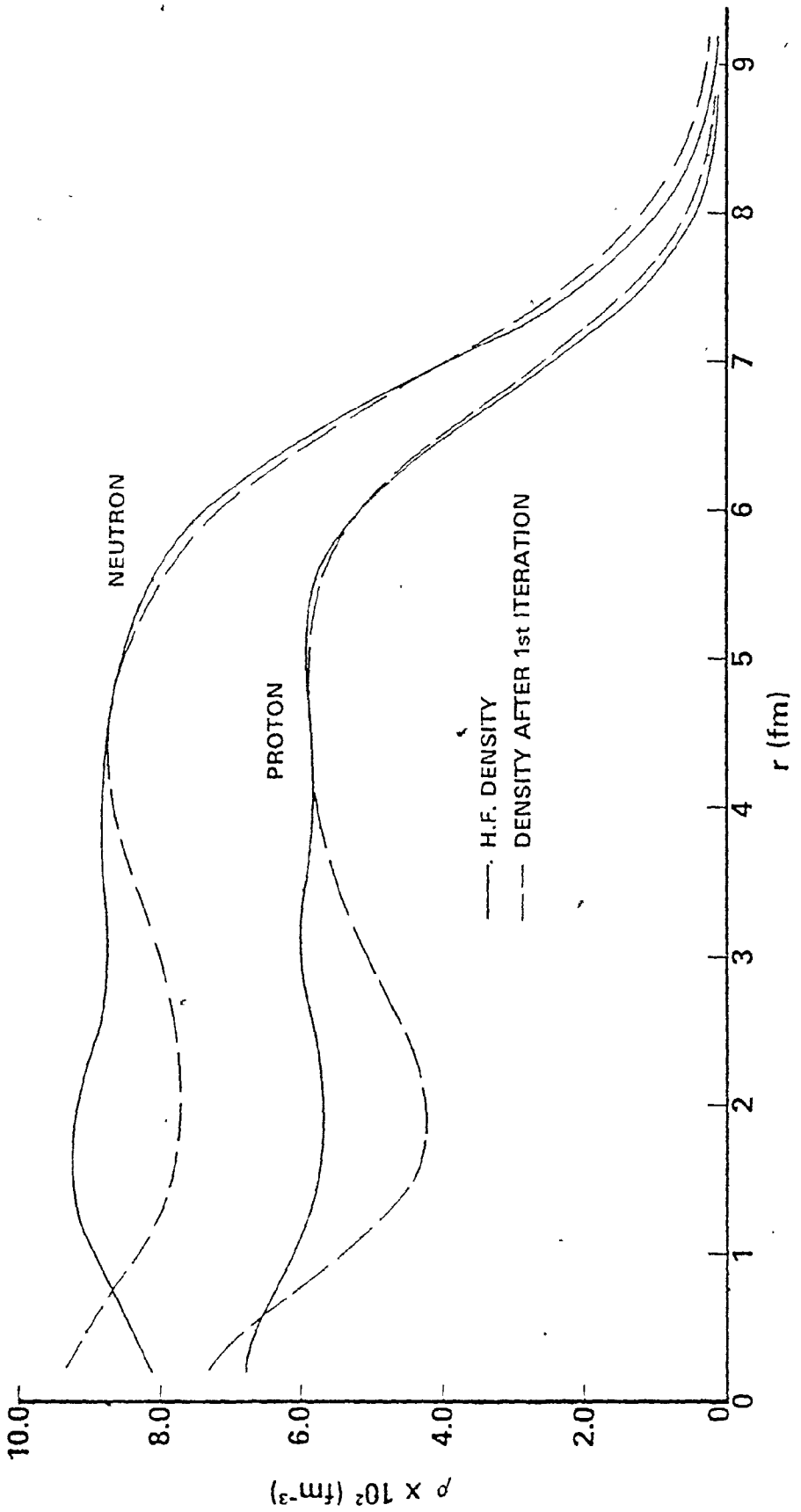
NEUTRON
PROTON
H.F. DENSITY
DENSITY AFTER 1st ITERATION
r (fm)
ρ x 10² (fm⁻³)
0
1
2
3
4
5
6
7
8
9
2.0
4.0
6.0
8.0
10.0

CHAPTER III

DEFORMED NUCLEI

Hartree-Fock calculations performed with density dependent effective interactions have been quite successful in describing the static properties of spherical nuclei[6,21]. Since the basic ingredients of such interactions do not depend on the specific nuclear system considered, extension of HF calculations to deformed nuclei should be easy. In particular, the constrained Hartree-Fock (CHF) technique developed by Flocard et al.[9] has been even used for fission barrier calculations and for predicting the properties of superheavy nuclei. Although the analytical simplicity of Skyrme interaction, which has been most used in CHF calculations, makes the numerical computations easier, it still takes thirty or more iterations for a given deformation of a moderately heavy nucleus to achieve self-consistency in both the energy and in the quadrupole moment. In view of such large computer time involved, one might be willing to sacrifice some accuracy in HF results for substantial saving in computer time. Strutinsky-type calculations[15,22] are faster to implement in deformed nuclei but they are not microscopic in nature. The TSIM discussed in sec. II.1 fills this gap. Although the basic approximation remains the same, some modifications are necessary to

implement a constrained calculation and to include pairing correlations. We discuss the implementation of constraints in sec. III.1. Since our method is not a self-consistent one, the number of degrees of freedom included in the deformation of the starting field is very important as has been emphasized by the Strutinsky-type calculations[22]. We discuss the details of such procedure in sec. III.2. Effects of pairing correlations in CHF calculations are generally included in the BCS approximation. Correction to our estimate of the total energy due to pairing is discussed in sec. III.3. Since the HF solutions for deformed nuclei are obtained by projection of the single particle states on to a truncated basis, the final results are dependent on the basis parameters[9]. The energy obtained is always a lower bound to the exact HF energy. Therefore a judicious choice of basis parameters is necessary. Details of these are contained in sec. III.4. In sec. III.5 two deformed nuclei, ^{134}Ce and ^{168}Yb, from two different regions of the periodic table are taken as illustrative examples and results from the TSIM are compared with the corresponding CHF results.

III.1 Constraints

One of the purposes of performing the HF calculations in deformed nuclei is to study the variation of the binding energy with deformation. To do so, one must add an external field to the Hamiltonian H. One generally constrains the sys-

tem to have a specific value of the quadrupole moment $\langle Q \rangle$ by minimizing[9)]

$$\langle H \rangle + f(\lambda, \langle Q \rangle)$$

where λ is a constant and f is a differentiable function of λ and $\langle Q \rangle$. The energy E of the system, which is called the "constrained Hartree-Fock" (CHF) energy is then simply $\langle H \rangle$. The constraint can be chosen in different forms; the linear constraint where

$$f(\lambda, \langle Q \rangle) = \lambda \langle Q \rangle \ ,$$

and the quadratic constraint where

$$f(\lambda, \langle Q \rangle) = \frac{1}{2} k (\langle Q \rangle - \lambda)^2 \ .$$

For a full CHF calculation, since one does not solve for the Lagrange multiplier λ, it has been emphasized by Flocard et al.[9)] that the quadratic constraint is the most practical to use. However, as will be mentioned later, we have found that the modifications in TSIM through a linear or a quadratic constraint yield similar results. Therefore, all our calculations have been performed with linear constraint.

For deformed nuclear calculations, the TSIM has to be modified slightly. If ρ is the self-consistent density, then the constrained energy is

$$E(\lambda) = \mathrm{tr}_1 \hat{t}_1 \rho_1 + \frac{1}{2}\,\mathrm{tr}_1\mathrm{tr}_2 \rho_1\rho_2 v_{12} + \lambda\,\mathrm{tr}_1 \hat{Q}_1 \rho_1, \qquad (3.1)$$

where $\hat{Q} = \sum_{i=1}^{A} \hat{Q}_i$, $\hat{Q}_i$ being the quadrupole moment operator for the ith particle. If the trial density is $\rho^{(0)}$, then

$$E(\lambda) = E^{(0)}(\lambda) + \mathrm{tr}_1 (\hat{t}_1 + U_1^{(0)}(\lambda))\delta\rho_1 + \frac{1}{2}\,\mathrm{tr}_1\mathrm{tr}_2 \delta\rho_1\delta\rho_2 v_{12} ,$$

where $\delta\rho = \rho - \rho^{(0)}$. Here the one-body field $U_1^{(0)}(\lambda)$ is modified to

$$U_1^{(0)}(\lambda) = \mathrm{tr}_2 \rho_2^{(0)} v_{12} + \lambda \hat{Q}_1 ,$$

and the zeroth iteration energy is

$$E^{(0)}(\lambda) = \mathrm{tr}_1 \hat{t}_1 \rho_1^{(0)} + \frac{1}{2}\,\mathrm{tr}_1\mathrm{tr}_2 \rho_1^{(0)}\rho_2^{(0)} v_{12} + \lambda\,\mathrm{tr}_1 \hat{Q}_1 \rho_1^{(0)} .$$

The quadrupole moment $Q^{(0)}$ generated by $\rho^{(0)}$ is simply $\mathrm{tr}_1 \hat{Q}_1 \rho_1^{(0)}$. If $\rho^{(1)}$ is the density generated through the field $U_1^{(0)}(\lambda)$, then the corresponding quadrupole moment $Q^{(1)}$ will be $\mathrm{tr}_1 \hat{Q}_1 \rho_1^{(1)}$. Since we estimate the HF energy at a given deformation, we require that $Q^{(1)} = Q^{(0)}$. This is done by adjusting the value of the Lagrange multiplier λ. In practice, one has to perform calculations with two different values of λ and evaluate the values of the quadrupole moment after one iteration. For linear constraint, it is found that this quadrupole moment changes almost linearly with λ (when pairing correlations are included), so that the optimum value of λ

that would yield a quadrupole moment $Q^{(1)}$ equal to $Q^{(0)}$ can be easily estimated. With this choice of λ, the density $\rho^{(1)}$ is calculated. In our approximation then

$$E(\lambda) \approx E^{(0)}(\lambda) + \mathrm{tr}_1(\hat{t}_1+U_1^{(0)}(\lambda))(\rho_1^{(1)}-\rho_1^{(0)}) ,$$

where the appropriate terms mentioned in sec. II.1 have been neglected. Thus our estimate for the CHF energy for a given $Q^{(0)}$ is

$$E_{CHF} \approx E^{(0)}(\lambda) + \mathrm{tr}_1(\hat{t}_1+U_1^{(0)}(\lambda))(\rho_1^{(1)}-\rho_1^{(0)}) - \lambda\, \mathrm{tr}_1\rho_1^{(0)}\hat{Q}_1 . \quad (3.2)$$

III.2 Deformation of the starting field

It was mentioned in sec. II.3b that we have preferred to use Woods-Saxon wave functions over the harmonic oscillator wave functions to generate the trial density $\rho^{(0)}$ because the neglected terms in our approximation are individually found to be small for the former choice. For deformed nuclear calculations, the Woods-Saxon potential V(r) must be deformed with a certain prescription. For small changes from the sphericity, it is sufficient to introduce only ellipsoidal deformations, which is done by defining the variable $r = \sqrt{r_\perp^2 + \delta z^2}$, where $r_\perp$ is the perpendicular distance from the z-axis of symmetry and δ is a deformation parameter. However, for large deformations the HF minimum valley lies far away from the ellipsoidal shape. This was recognized by Brack et al.[22] while performing Strutinsky-type calculations for fission barriers of actinides. The

nuclear shape at large deformations must be parametrized in such a way so as to produce a neck. Damgaard et al.[23] have suggested that one can assume a surface π, which up to a scale factor describes the shape of the nuclear surface by

$$\pi(\beta,u,v) = 0 \ , \tag{3.3}$$

where β is a set of deformation parameters, and u and v are dimensionless coordinates proportional to the ordinary cylindrical coordinates

$$u = z/C \ ,$$

and $$\tag{3.4}$$

$$v = r_{\perp}/C \ .$$

We present here some details of such parametrization. The origin of the coordinate system coincides with the centre of mass of the assumed shape. C in eqn. (3.4) is determined through the condition of volume conservation

$$C = R_0 \left[\frac{3}{4} \int_{u_1}^{u_2} v^2(u)\,du\right]^{-1/3} \tag{3.5}$$

where u_1 and u_2 are the two end points where v(u) becomes zero and R_0 is the radius of the nucleus in spherical shape. The radial dependence of the potential V is expressed in terms of a single variable ℓ which is a function of z and $r_{\perp}$

$$V(\ell) = V(z,\rho) \ .$$

In particular, for Woods-Saxon potential

$$V(\ell) = - \frac{V_0}{1+\exp(\ell/a)} \qquad (3.6)$$

where "a" is the diffuseness parameter. One assumes that the nuclear surface is also an equipotential surface where $\ell(z,r_\perp) = 0$ is satisfied. The function ℓ is chosen by assuming that the normal derivative of the potential is of constant magnitude all along the nuclear surface. This ensures the skin thickness to be constant as the nucleus is deformed. Thus

$$\ell(u,v) = \frac{C\pi(u,v)}{|\nabla_{u,v}(\pi(u,v)|} , \qquad (3.7)$$

which is positive outside and negative inside the potential surface. A definition of π that has been widely used[22,24] is

$$\pi(u,v) = v^2 - (1-u^2)(A+Bu^2+\alpha u) , \qquad (3.8)$$

where α describes the asymmetry in the z-direction. When $\alpha = 0$, π defines a number of shapes, varying from spherical ($B = 0$, $A = 1$) to two fragment configurations ($A < 0$). When $\alpha = B = 0$ and $A > 0$, one gets ellipsoidal shapes. Also, $B < A$ defines one-centre shapes whereas $B > A$ defines two-centre shapes. Since the parameters A and B have no direct physical meaning, one defines a new set of parameters (c,h) where c is a dimensionless parameter

$$c = C/R_0$$

so that 2c is the total length of the longer axis in units of

R_0. The parameter h is a measure of variation of the thickness of the neck. Some axially symmetric shapes as a function of c and h are shown in Fig. 2. For the definition of π in eqn. (3.8), the values of u_1 and u_2 in eqn. (3.5) are -1 and +1 respectively. The scale factor c is then

$$c = (A + \frac{1}{5} B)^{-1/3} .$$

The parameter h is chosen in such a way that $n = 0$ line approximately fits the bottom of the liquid-drop valley. Thus,

$$\begin{aligned} B &= 2h + \frac{1}{2} (c-1) \\ A &= \frac{1}{c^3} - \frac{1}{5} B . \end{aligned} \tag{3.9}$$

In terms of the new set, the spherical shape is given by $c = 1$ and $h = 0$.

With the definition of ℓ in eqn. (3.7), one does not get back the Woods-Saxon potential in the spherical limit. One therefore defines a function $\Pi(u,v)$, which will generate the same shapes as the function π and at the surface will satisfy $\Pi(u,v) = 0$, as

$$\Pi(u,v) = [\pi(u,v) - \pi_{min}]^{\frac{1}{2}} - [-\pi_{min}]^{\frac{1}{2}} , \tag{3.10}$$

where π_{min} is the minimum value of $\pi(u,v)$. For one centre shapes where $A > B$,

$$\pi_{min} = -A , \tag{3.11}$$

Fig. 2 Some axially symmetric shapes[22] in the (c,h) parametrization (eqn. 3.8). The dotted curves correspond to $\alpha \neq 0$. In all the TSIM calculations here $h = \alpha = 0$ shapes have been considered.

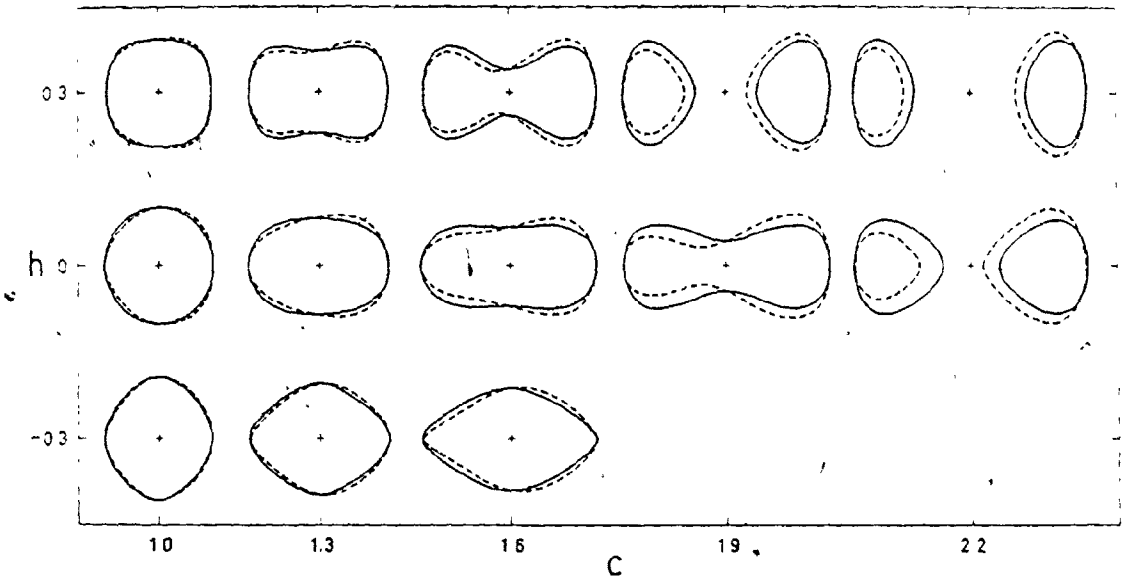
0 3
h 0
-0 3
1 0
1.3
1 6
1 9
2 2
C

and for two-centre shapes where A < B

$$\pi_{min} = -\frac{1}{4}\left[(A+B)^2/B\right] . \qquad (3.12)$$

The function ℓ is redefined as

$$\ell = \frac{cR_0\Pi(u,v)}{|\nabla_{u,v}\Pi(u,v)|} . \qquad (3.13)$$

With this definition, ℓ reduces to the variable $r - R_0$ in the spherical limit. Thus, for a given c and h, the values of A and B are determined from eqn. (3.9) which in turn can be used to define $\Pi(u,v)$ in eqn. (3.10) and hence ℓ in eqn. (3.13). This defines the Woods-Saxon potential in eqn. (3.6).

III.3 Pairing energy

A detailed microscopic description should take into account the effects of both short range and long range correlations. Pairing correlation is an example of the latter type. Such correlations play an important role in deformed nuclei because the single particle density of states near the Fermi surface is large. Inclusion of pairing in a self-consistent way is equivalent to the Hartree-Fock-Bogolyubov (HFB) approximation where the solutions are far more difficult to obtain than in the usual HF approximation. Such calculations have been done by Gogny and collaborators[25,26] with finite range forces. However, the way Skyrme interaction has been constructed, a correct description of pairing through the interaction is not possible. Therefore, one performs a HF plus BCS type

calculation. Such a scheme has been formulated by Vautherin[7] and implemented in CHF calculations by the Orsay group[9]. Instead of the HF energy in sec. II.2, one minimizes the quantity

$$E = \int d\underset{\sim}{r}\, H(\rho,\tau,\underset{\sim}{J}) - \frac{G}{2}\left(\sum_i u_i v_i\right)^2 , \qquad (3.14)$$

where G is the pairing strength and v_i^2 is the occupational probability of the ith orbit. E is minimized with the conditions

$$u_i^2 + v_i^2 = 1$$

$$\sum_{i=1}^{\infty} v_i^2 = A$$

and $$\int d\underset{\sim}{r}\,|\phi_i^2(\underset{\sim}{r})|^2 = 1 .$$

The various densities are defined accordingly

$$\rho(\underset{\sim}{r}) = \sum_{i=1}^{\infty} v_i^2 |\phi_i(\underset{\sim}{r})|^2 ,$$

and likewise for $\tau(\underset{\sim}{r})$ and $\underset{\sim}{J}(\underset{\sim}{r})$ defined earlier in eqn. (2.10).

Minimization of E leads to two sets of coupled equations, the first one being the usual HF equations and the second one is the set of BCS equations. The condensation energy E_p, which is added to the energy of the nucleus obtained from the HF equations, is then

$$E_p = -\frac{\Delta}{2} \sum_i u_i v_i \quad ,$$

where the gap Δ is related to the pairing strength G by

$$\Delta = G \sum_i u_i v_i \quad .$$

In performing a HF+BCS calculation, one has various choices for G or Δ at disposal. We have assumed a constant Δ, independent of deformation. For large deformations, this prescription gives better agreement with the realistic HFB calculations of Gogny and collaborators[25,26], than, for example, a pairing interaction G proportional to the surface area. In the TSIM, starting with a given deformation of the Woods-Saxon potential and a strength parameter $G^{(0)}$, a BCS calculation yields probability amplitudes $u_i^{(0)}$ and $v_i^{(0)}$ and a gap

$$\Delta = G^{(0)} \sum_i u_i^{(0)} v_i^{(0)} \quad .$$

In the next iteration the gap Δ is kept fixed by letting $G^{(0)}$ change to $G^{(1)}$; that is, a new set of $u_i^{(1)}$ and $v_i^{(1)}$ gives

$$\Delta = G^{(1)} \sum_i u_i^{(1)} v_i^{(1)} \quad .$$

Writing the amplitudes $u_i^{(1)} = u_i^{(0)} + \delta u_i$ and $v_i^{(1)} = v_i^{(0)} + \delta v_i$ and neglecting second order terms $\delta u_i \delta v_i$, the change in condensation energy is

$$E_p^{(1)} - E_p^{(0)} \approx E_p^{(0)} \frac{G^{(0)} - G^{(1)}}{G^{(1)}} \quad . \qquad (3.15)$$

This term should be added to eqn. (3.2), keeping in mind that $E^{(0)}(\lambda)$ already includes $E_p^{(0)}$ and the densities have been calculated with proper occupational probabilities.

In our calculations the gap Δ has been taken to be 1 MeV for ^{134}Ce in accordance with the corresponding CHF calculation. For all other nuclei the gap has been taken equal to $12\ A^{-\frac{1}{2}}$.

III.4 Choice of the basis

Vautherin[7] has formulated in detail the solution of the HF equations by expanding the single-particle wave functions in the basis of an axially symmetric deformed oscillator[23]. The Hamiltonian is diagonalized in each subspace with good quantum number Ω and parity. Since axial symmetry is assumed, one needs to calculate two dimensional integrals, the two variables being z and $r_\perp$. Owing to the reflection symmetry, the two variables have limits 0 and $+\infty$. The integration in the z-direction is performed with 20 points Gauss-Hermite formula and the integration in $r_\perp$ is done with 10 points Gauss-Laguerre formula.

Since in practice one cannot use a complete basis set to expand the HF states, only a limited number of basis states can be retained depending upon the limitations of the computer. It is convenient to use an energy-dependent cut-off[9,23]. This means that for a given deformation, all basis states are used which come down within a certain specified energy.

In the usual notation, the basis states included obey the condition[9]

$$\hbar\omega_\perp(n_\perp+1) + \hbar\omega_z(n_z + \tfrac{1}{2}) \leq \hbar\omega_0(N+2) \ , \tag{3.16}$$

where $\hbar\omega_0 = \hbar(\omega_z\omega_\perp^2)^{1/3}$ and $n_\perp = 2n_{r_\perp} + \Lambda$. Here $n_{r_\perp}$ and n_z are the number of nodes in the $r_\perp$ and z directions and Λ is the projection of orbital angular momentum on the z-axis. We have taken N = 8 and 10 for ^{134}Ce and ^{168}Yb respectively. Due to computer restrictions, we have limited the value of $n_{r_\perp}$ by the condition

$$n_{r_\perp} = N_{cut}/2 \ , \tag{3.17}$$

with N_{cut} equal to 12 for Ce and 16 for Yb.

The oscillator basis has two parameters $\omega_\perp$ and ω_z. For ellipsoidal deformations one defines a parameter $q_{basis} = \omega_\perp/\omega_z$. Since the HF solutions are obtained with a limited basis, it is important to optimize the values of q_{basis} and the equivalent oscillator parameter $b = \sqrt{m\omega_0/\hbar}$. Following Flocard et al.[9], given a deformation q of the Woods-Saxon potential the value of q_{basis} is adjusted to yield a quadrupole moment Q equal to that of a rotationally symmetric ellipsoid given by

$$Q = \frac{2}{3} Ar_0^2 q^{-2/3}(q^2-1) \ ,$$

where $r_0 = 1.2049\ A^{1/3}$ fm. The optimum value of b is

$$b = \alpha' q^{1/3}\left(\frac{3}{2+q^2}\right)^{\frac{1}{2}} \ ,$$

where the constant α' is equal to the value of b which minimizes the sum of occupied single particle energies for the Woods-Saxon field at q = 1. This procedure has been used to determine q_{basis} and b for ^{134}Ce.

For very large deformation, we deform the Woods-Saxon potential according to the (c,h) parametrization discussed in sec. III.2. The q_{basis} in such a case is

$$q_{basis} = \sqrt{\langle z^2 \rangle / \langle \tfrac{1}{2} r_\perp^2 \rangle}$$

For the liquid drop type density, Brack[27] estimates

$$q_{basis} = c^{3/2}[1+6x-6x^2+O(x^3)+\cdots] \qquad (3.18)$$

with

$$x = \frac{1}{35} c^3 [2h + \frac{1}{2}(c-1)] \ .$$

The parameter b is adjusted to yield a minimum for the sum of the occupied single particle energies. This procedure has been adopted for Yb and for fission barrier calculations of actinides for h = 0. For small deformations, the two procedures mentioned above yield similar results.

III.5 Results for ^{134}Ce and ^{168}Yb

We now compare the results of our calculations with the corresponding CHF ones for two medium mass nuclei. The CHF calculation for ^{134}Ce was done by Flocard et al.[9] with

Skyrme II force and we use the same force for comparison. Fig. 3 displays the energy versus quadrupole moment curves obtained by the two methods. Although our method overshoots the CHF curve by a few MeV, the deformation energy is remarkably well reproduced over the entire range. It should be mentioned here that the CHF curve is obtained using a quadratic constraint as opposed to the TSIM which uses a linear constraint. Once the optimum values of the basis parameters q_{basis} and b are determined for each deformation, only three iterations are needed to choose the appropriate value of the Lagrange multiplier λ as mentioned in sec. III.1. In contrast, about thirty or more iterations are needed for each deformation in the CHF curve.

We compare our results for ^{168}Yb with the CHF calculations[27] in Fig. 4 using Skyrme III force. In this case the TSIM energy underestimates the CHF energy by about 15 MeV. However, our estimate for Yb does not include the centre-of-mass correction which the CHF curve does. Since the HF Slater determinant is not an eigenstate of the total momentum $\underset{\sim}{P}$, the HF energy can be corrected by approximately subtracting the mean energy of the centre-of-mass motion[19]

$$E_{cm} = \langle \underset{\sim}{P}^2 \rangle / 2mA$$

where $\underset{\sim}{P} = \sum_{i=1}^{A} \underset{\sim}{p}_i$. However, generally the two-body part of the $\underset{\sim}{P}^2$ operator is neglected in calculations. The required correction given by only the one-body part is then

Fig. 3 Deformation energy of ^{134}Ce as a function of the mass quadrupole moment using the Skyrme II interaction. The dashed line represents the TSIM result, whereas the full line corresponds to the CHF calculation[9]. Pairing energy is included with a constant gap $\Delta = 1$ MeV.

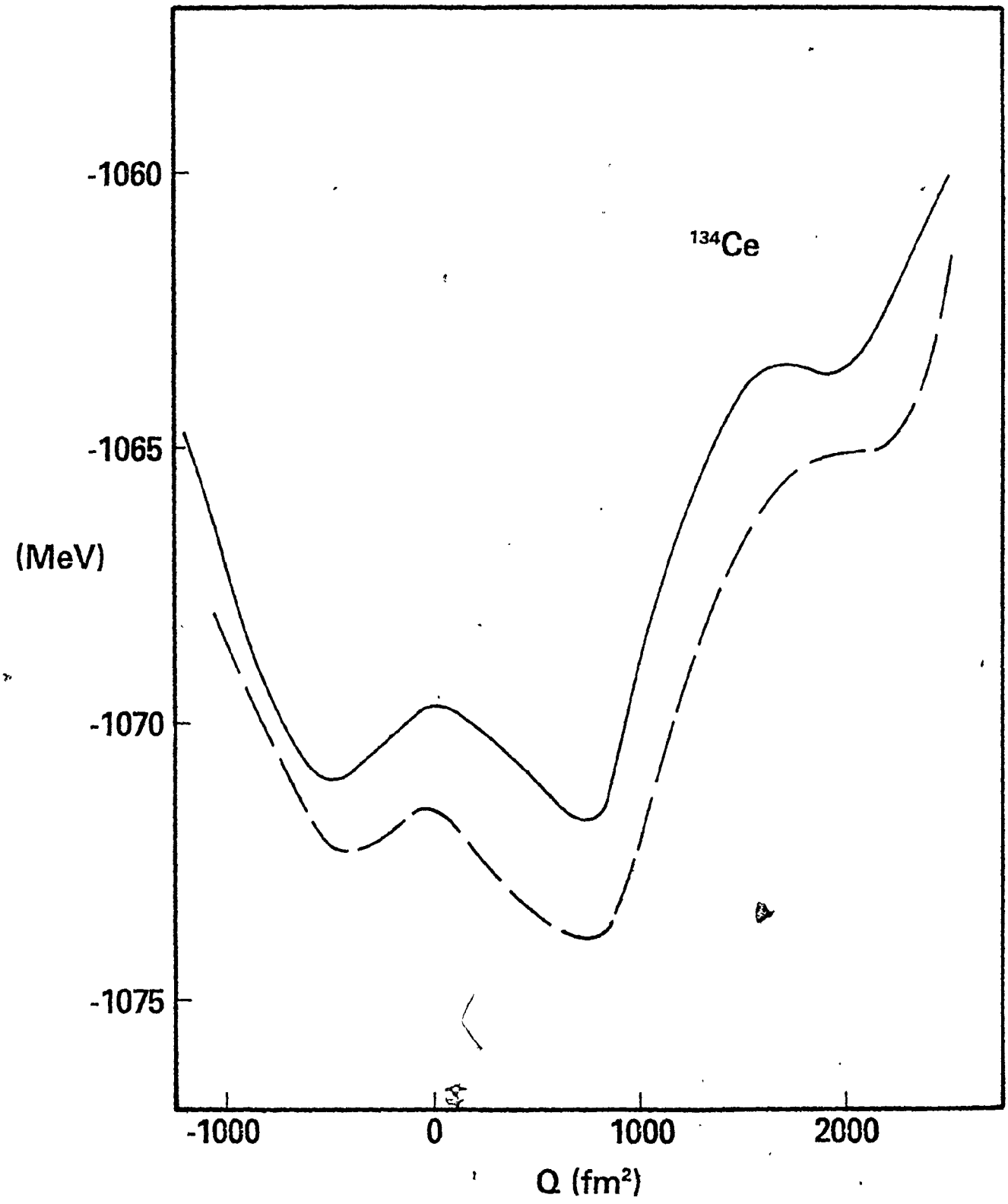
-1060
-1065
-1070
-1075
(MeV)
^{134}Ce
-1000
0
1000
2000
Q (fm^2)

Fig. 4 Comparison of zeroth order energy $E^{(0)}$ and our estimate $E^{(0)} + \Delta E^{(1)}$ as a function of Q with the CHF calculations[27] for ^{168}Yb. Calculations were done with the Skyrme-III interaction. The continuous line is the CHF result. The dot-dash curve is the zeroth order estimate $E^{(0)}$ and the dashed curve is the TSIM estimate. A constant gap $\Delta = 12\ A^{-\frac{1}{2}}$ MeV has been taken for pairing calculations. The CHF calculation includes the centre-of-mass correction whereas the TSIM estimate does not.

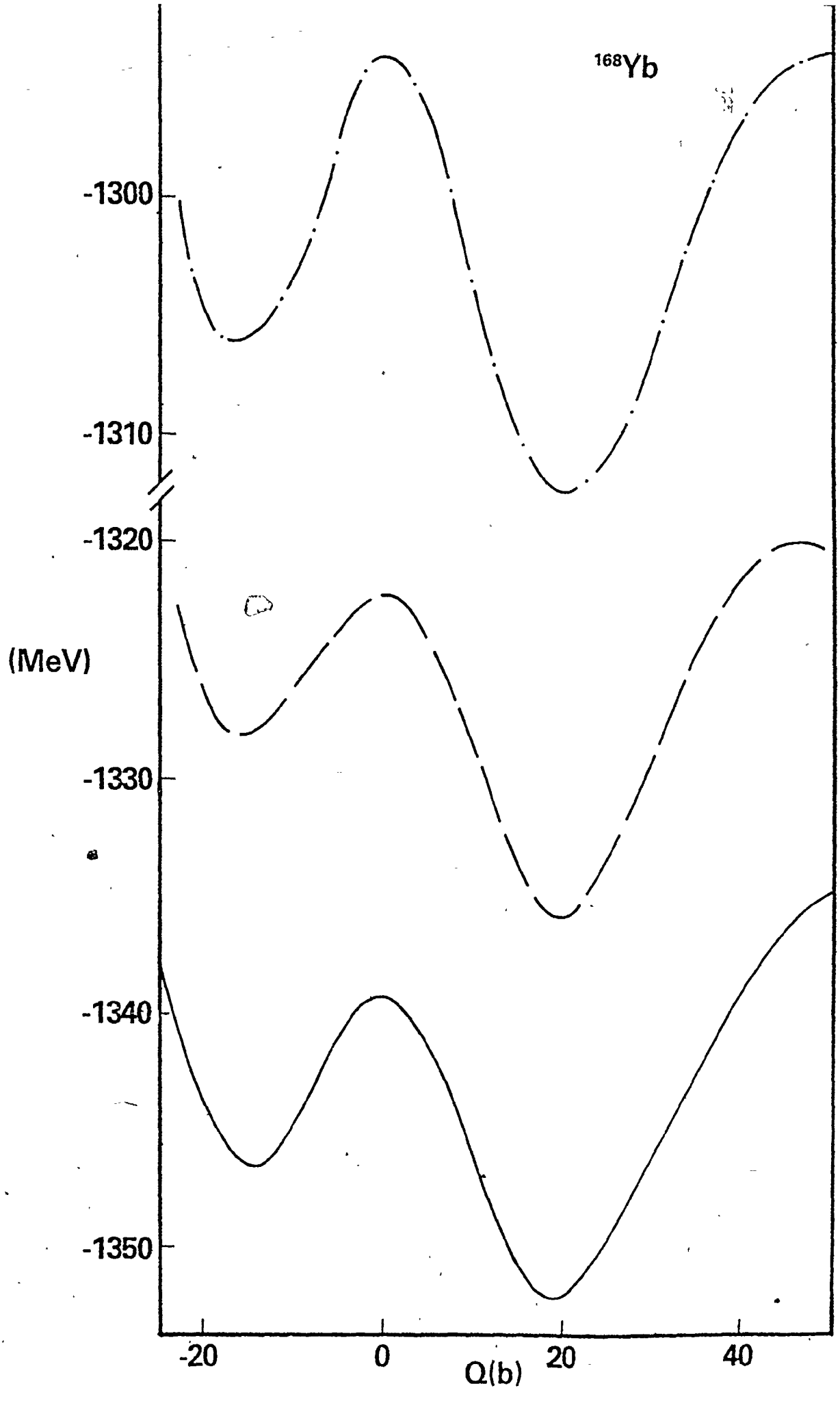
^{168}Yb
-1300
-1310
-1320
-1330
-1340
-1350
(MeV)
-20
0
20
40
Q(b)

$$E^0_{cm} = \langle \sum_i \underset{\sim}{p}_i^2 \rangle / 2mA \ .$$

The effect of this correction is to replace the nucleon mass m by mA/(A-1) in the total kinetic energy. We have checked that inclusion of one-body part of the centre-of-mass correction only changes the energy scale of TSIM results. For ^{168}Yb this correction is about 15 MeV which accounts for the difference in energy betweem the TSIM and the CHF results. We plot in the same figure, the zeroth order estimate $E^{(0)}$, the first term in eqn. (3.2). Our final results are very similar to the "Expectation value method (EVM)" of Brack[27]. The latter[28] is simply the evaluation of $E^{(0)}$, but using a carefully chosen deformed Woods-Saxon potential. The parameters of such a potential for a given nucleus are obtained by performing a spherical HF calculation and by approximating the self-consistent potential by the Woods-Saxon potential. The deformations are determined from the corresponding Strutinsky calculations. It was also essential in Brack's calculation[27] to introduce a sophisticated r-dependence in the effective mass. In practice, a judicious choice of the one-body potential is vital for the success of EVM, and this has to be done for each nucleus. On the other hand, we generate $\rho^{(0)}$ through a simple Woods-Saxon potential whose parameters are fixed, and take the effective mass to be unity. Our zeroth order estimate $E^{(0)}$ is therefore worse than Brack's, but the correction term obtained through one iteration corrects adequately for this deficiency.

Although the TSIM works reasonably well to reproduce the energy versus deformation curve, it does not provide us

with an accurate density profile as we have noted in the calculations for spherical nuclei. However, the density $\rho^{(1)}$ after one iteration is closer to ρ_{HF} than $\rho^{(0)}$. This can be seen in Fig. 5 which shows that $\rho^{(1)}$ yields the right dependence of the root mean square radius to the quadrupole moment for ^{134}Ce.

Fig. 5 Variation of the root mean-square charge radius of ^{134}Ce as a function of the quadrupole moment. The dashed curve represents the TSIM result and the continuous line corresponds to the CHF calculation[9].

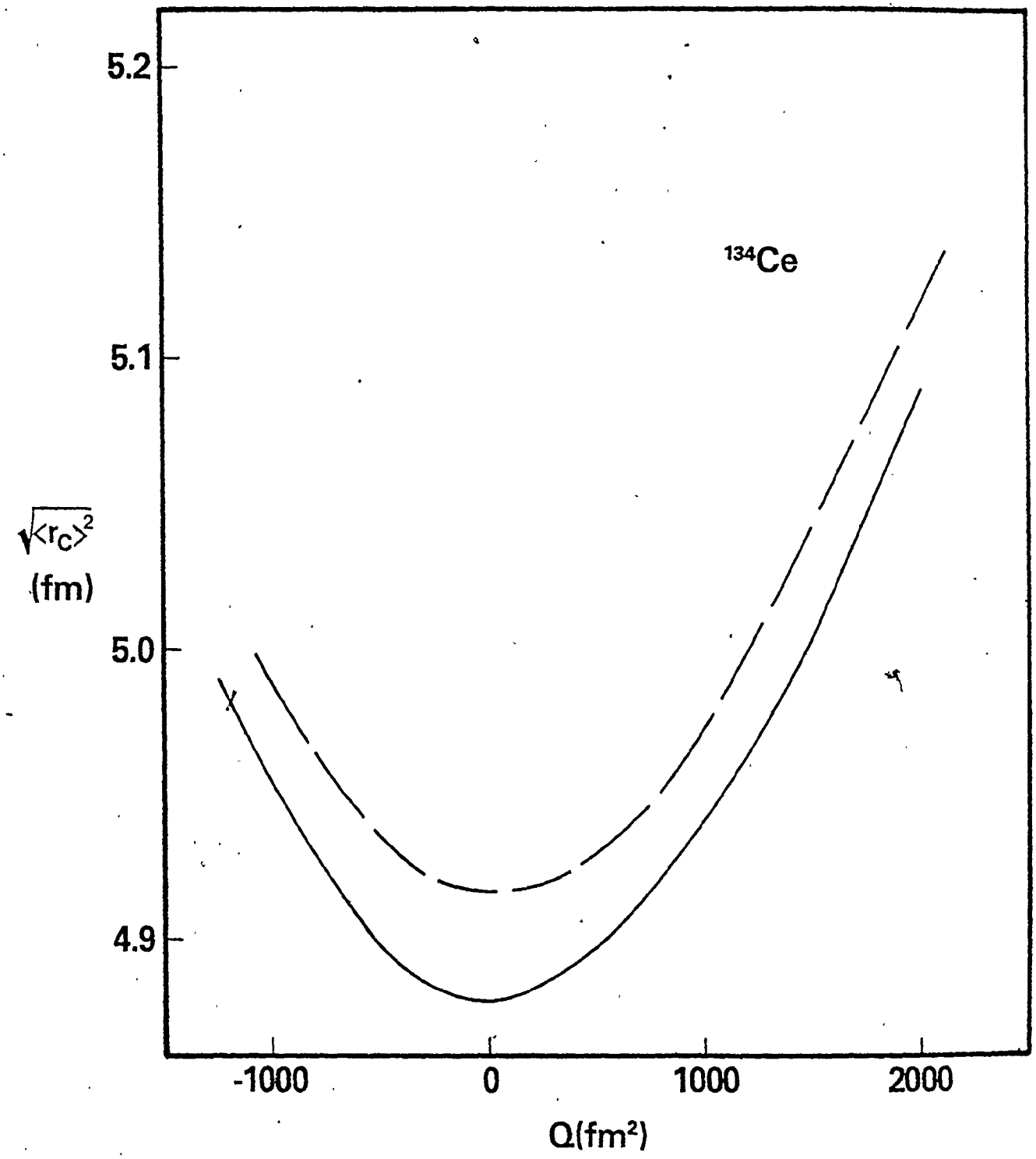
5.2
5.1
5.0
4.9
$\sqrt{\langle r_c \rangle^2}$
(fm)
^{134}Ce
-1000
0
1000
2000
Q(fm^2)

CHAPTER IV

FISSION BARRIERS

IV.1 Introduction

Since the discovery by Hahn and Strassmann[29] that uranium when bombarded with neutrons, split into lighter elements with about half the atomic number of uranium, an enormous amount of experimental information on nuclides undergoing such a process has been accumulated. Fission is a branch of nuclear physics which has developed almost independently of the rest of nuclear physics. The models used in correlation of fission data are crude compared to the models for nuclear structure calculations. This is because fission is an extremely complex phenomenon. In nuclear structure calculations one may have to deal with only a few outermost nucleons involving a small amount of energy. In contrast, fission deals with cataclysmic rearrangement of two nearly equal mass nuclei in a nucleus involving a large amount of energy which in turn affects the motion of individual nucleons.

The time period within which fission takes place can be divided into two intervals. During the first interval of time ($\sim 10^{-15}$ s) which is large compared to the characte-

ristic nuclear time ($\sim 10^{-22}$ s) the energy imparted to the nucleus is redistributed among the nucleons involving many nuclear collisions. This energy goes into the collective degrees of freedom thus causing the nucleus to deform. If no nucleons gain enough energy to escape, the nucleus keeps deforming up to a critical point called saddle point, at which it is unstable. Shape instability then sets in and in the much shorter second interval of time ($\sim 10^{-21}$ s) the nucleus reaches the point of scission.

There are two aspects of fission problem: the statics and the dynamics. Static means that the nucleus is in a shape of equilibrium and therefore the study of potential energy surfaces becomes useful. The dynamics of the problem where the equations of motion are to be solved should be definitely considered from saddle point to scission in the fission process since the separation of collective and intrinsic coordinates is not meaningful. We shall be interested here in statics of fission. Static calculations fall into two categories: adiabatic and non-adiabatic. If the collective motion towards scission is sufficiently slow or the coupling to internal degrees of freedom sufficiently weak so that the single particle degrees of freedom can easily readjust to each new deformation, then the adiabatic limit is valid. In this case, the decrease in potential energy from saddle to scission appears in the collective degrees of freedom, mainly as the relative kinetic energy of nascent fragments. The

opposite situation occurs if the coupling is strong enough to transfer some collective energy into individual nucleonic excitations. Such a transfer gives rise to nuclear viscosity and the relative kinetic energy of fragments is reduced. In this case a non-adiabatic treatment is more appropriate. We shall restrict ourselves to a brief survey of calculations in the adiabatic limit.

The earliest adiabatic model of fission, the liquid drop model (LDM), was proposed by Bohr and Wheeler[30]. The idea was to replace the actual Hamiltonian of the nucleus with a model containing a simple classical Hamiltonian; in this case that of a charged incompressible drop of liquid. The stability of a nucleus against distortions is governed by the interplay between the surface energy and the Coulomb energy. If a nucleus is distorted from its equilibrium shape, the surface energy increases by ΔE_s and the Coulomb energy decreases by ΔE_c. The sum $\Delta E_s + \Delta E_c$ must be positive for guaranteeing the stability against distortions. The stability against deformation is determined by the fissility parameter $\chi = E_c^o/2E_s^o$, where E_c^o and E_s^o correspond to the Coulomb and surface energies of the spherical drop. For χ less than unity, the drop is stable although fission through barrier penetration is possible. If χ is greater than unity, then there is no potential barrier to inhibit the nucleus to undergo spontaneous fission.

A great deal of work[31] has been done in calculating

potential energy surfaces of drop shapes other than ellipsoidal distortions. For $\chi > 0.39$, the nucleus was shown to be unstable against symmetric deformation although it was stable against asymmetric distortions. This preference of the LDM to symmetric mass fission is in general contrary to the experimental findings. Besides this disagreement between the LDM and experiments, the predicted barrier heights are much higher. Also the inadequacy of LDM is realized by the fact that not all nuclei are spherical in their ground state. The LDM favours a spherical ground state.

The failure of LDM has been due to neglect of shell-effects. The surface and Coulomb energies in a heavy nucleus are of the order of a few hundred MeV. The fact that fission barriers are only a few MeV, suggests a nearly complete cancellation between changes in the two energies. This means that those effects which can contribute a few MeV to the system cannot be neglected. Such a contribution comes from the fluctuation of single particle level density with deformation. Also, some levels may come down or go up in energy as the deformation proceeds. This shell effect arises due to the discreteness of individual particles. According to Strutinsky[14] the total energy E of the nuclear system can be regarded as

$$E = E_{macroscopic} + E_{microscopic},$$

where $E_{macroscopic}$ is the smoothly varying part of the total energy and is taken to be the liquid drop energy. $E_{microscopic}$

is the contribution from the shell and pairing corrections. If n_i is the occupational probability of ith level then

$$E_{shell} = 2 \sum_i e_i n_i - 2 \sum_i e_i \tilde{n}_i$$

and

$$E_{pair} = G \sum_i u_i v_i - \tilde{E}_{pair} ,$$

where $2 \sum_i e_i \tilde{n}_i$ and $\tilde{E}_{pair}$ are smooth averages of the total single-particle energy and the total pairing energy respectively and are calculated through Strutinsky's prescription. These are supposed to be included in the macroscopic energy. G is the pairing strength and v_i^2 is the occupation probability of ith level. The contribution from the microscopic part can drastically change the LDM potential energy surface.

Following the shell-correction method (SCM), Möller and Nix[32] have looked into potential energy surfaces in deformation space. They considered three coordinates: the distance r between the centres of mass of the two fragments, σ_2 describing the amount of neck formation and the mass asymmetry coordinate $\alpha = (M_1-M_2)/M_0$ where M_1 and M_2 are the masses of fragments and $M_0 = M_1+M_2$. For each value of r and α, the potential energy was minimized with respect to σ_2. The energy surface thus generated was found to favour asymmetric division of fragments for the nuclei considered, in accordance with the experimental results. Further, it was found that correlation between the theoretical fragment mass ratios and the corresponding experimental ratios is good.

The achievement of SCM lies in the fact that it has been able to explain the experimental results quite well. The well known existence of double humped barriers in actinides has been explained by SCM. The theoretical barrier heights are within 1 or 2 MeV of experimental estimates in most cases. It also can predict ground states at finite deformation. Further, the final results are found to be close even when the Strutinsky averaging procedure is carried out starting with two different single particle potentials. Potential energy surfaces of a large number of actinides as well as superheavy elements have been obtained[15,33] by SCM because the method is fast to implement.

The dual approach taken in SCM has found some justification in the work of Brack and Quentin[34]. They have shown that the sum of Strutinsky average energy and the first order shell correction reproduces perfectly well the exact HF energy if the average density matrices are calculated self-consistently. Jennings and Bhaduri[35] have shown that the energy averaging in SCM is equivalent to an extended Thomas-Fermi approximation. However, since in SCM the one-body fields are chosen in an ad-hoc manner, it is preferable to perform a self-consistent calculation in order to get a connection between the self-consistent field and various properties of nuclei. Thus, one would like to trace deformation energy curves self-consistently too. In view of the difficulties mentioned in

sec. I.1, such calculations, at present, are performed within the Hartree-Fock approximation with effective forces and are few in number[12,13] because of the excessive computer time required. In this connection, a time saving approximation to the Hartree-Fock method developed by Ko et al.[28] and improved upon by Brack[27] has been useful. However, it is our contention that the TSIM is preferable because a careful selection of starting field is not required.

IV.2 Some methods of determination of fission barriers.

Fission barrier heights can be determined experimentally by reactions like (n,f), (d,pf), (t,pf) etc. The basic idea is to impart enough energy to the nucleus so that the barrier can be surmounted. However, fission is still possible through barrier penetration even if the excitation energy E_{ex} is less than the barrier height E_b, thereby making the estimation of E_b a little difficult. Below the barrier, the fission yield is expected to rise exponentially with increasing E_{ex} and for $E_{ex} > E_b$ the yield should level off. Such determinations of barrier heights have been made by Schmitt and Ruffield[36] using γ-rays to excite the nucleus. Fission can also be induced by exciting the target nucleus by monoenergetic neutrons. A zero energy neutron when captured gives an excitation energy B_n to the compound nucleus. Thus, if neutron with energy E_n is necessary to produce fission then the barrier $E_b = E_n + B_n$. This method will apply only when B_n is less than E_b which may

not be true for compound nuclei with an even number of neutrons. A way to get around this difficulty has been to use (d,pf) reaction[37]. The deuteron incident on a nucleus undergoes a stripping reaction whereby a proton is emitted. At a threshold energy E_d of deuteron, fission also takes place along the emission of proton of kinetic energy E_p. If the binding energy of a deuteron is B_d, then the captured neutron has an equivalent kinetic energy E_n, given by

$$E_d - E_p = B_d + E_n \ .$$

The barrier height E_b is then

$$E_b = E_n + B_n = (E_d - E_p - B_d) + B_n \ .$$

It can be seen that if all the kinetic energy is taken by the proton then $E_d - E_p < B_d$ and hence $E_b < B_n$.

It is possible that near the threshold energy, neutron emission also becomes possible. The competition between fission and neutron emission is governed by the ratio of widths Γ_f/Γ_n. The fission barrier is then estimated from some model calculation involving Γ_f/Γ_n which is related to the density of levels of the residual nucleus after neutron emission. The functional form for the density of levels is not unique. One such choice known as the Fermi-gas expression, where the level density is an exponential function of energy has been used[38] for barrier estimates of nuclei around mass number 180 which

exhibit single barrier. The situation is more complicated in actinides with double barrier because besides the possibility of prompt fission of compound nucleus, it can emit a neutron which will result in a residual nucleus in either the first well or the isomer well. A statistical model similar to that mentioned above, but with more parameters, has been used by Britt et al.[39,40] to estimate the heights of both barriers and that of the second minimum relative to the ground state in a large number of actinides.

IV.3 Fission barrier of ^{240}Pu

The method of estimating the results of a CHF calculation from the first two iterations of the HF cycle should be very useful in the actinide region. A CHF calculation for ^{240}Pu has been done by Flocard et al.[13] using Skyrme III. Since pairing correlations are not included in a self-consistent way, the choice of pairing strength in the HF+BCS calculation is important. Although there are no severe restrictions in the ground state because the pairing properties can be fitted reasonably well either with a constant Δ or G, the deformation dependence of these quantities is not well known. Flocard et al.[13] included pairing correlations with a strength G proportional to the surface area of an ellipsoidal liquid drop having the same quadrupole moment as the self-consistent solution. They find that the second barrier height is lower by about 8 MeV compared to the corresponding CHF calculation with a constant gap

$\Delta = 12\ A^{-\frac{1}{2}}$. At present, it is not conclusive to say which of these prescriptions is correct, although one can get some hints from the HFB calculations of Gogny[26] for ^{152}Sm. For large deformations where the second barrier occurs, the prescription of constant Δ gives better agreement with the HFB results. We have, therefore, chosen a constant Δ in our approximation.

In Fig. 6 we show the fission barrier result of ^{240}Pu from our approximation and compare it with the CHF result of the Orsay group as reproduced by Brack[27]. The number of basis states used in the expansion of single particle HF wave functions is governed by eqns. (3.16) and (3.17) where N = 12 and N_{cut} = 18. This choice of N underestimates the absolute HF energies for ^{240}Pu by about 8 MeV[41]. However, the shift in energy is uniform within 1 MeV even if one chooses a larger basis[13]. Thus, the basis size chosen for our calculation is reasonable for estimating barrier heights. The Coulomb exchange has been included in the Slater approximation given by eqn. (2.11). The starting Woods-Saxon potential has been deformed according to the (c,h) parametrization discussed in sec. III.2. The deformed potential has been restricted to follow the h = 0 line. A value of $c \approx 1.6$ is found sufficient for deformations up to the second barrier. One can see from the figure that the agreement between the CHF curve and our result is quite satisfactory, except that our second barrier

Fig. 6 The zero-order energy $E^{(0)}$ (dot-dash curve), the TSIM estimate $E^{(0)} + \Delta E^{(1)}$ (dashed curve) and the CHF fission barrier[27] (continuous curve) as functions of Q. Skyrme-III force has been used. Pairing calculations have been done with a constant gap $\Delta = 12\ A^{-\frac{1}{2}}$ MeV. The centre-of-mass correction is not included in the TSIM estimate, whereas it is included in the CHF calculation.

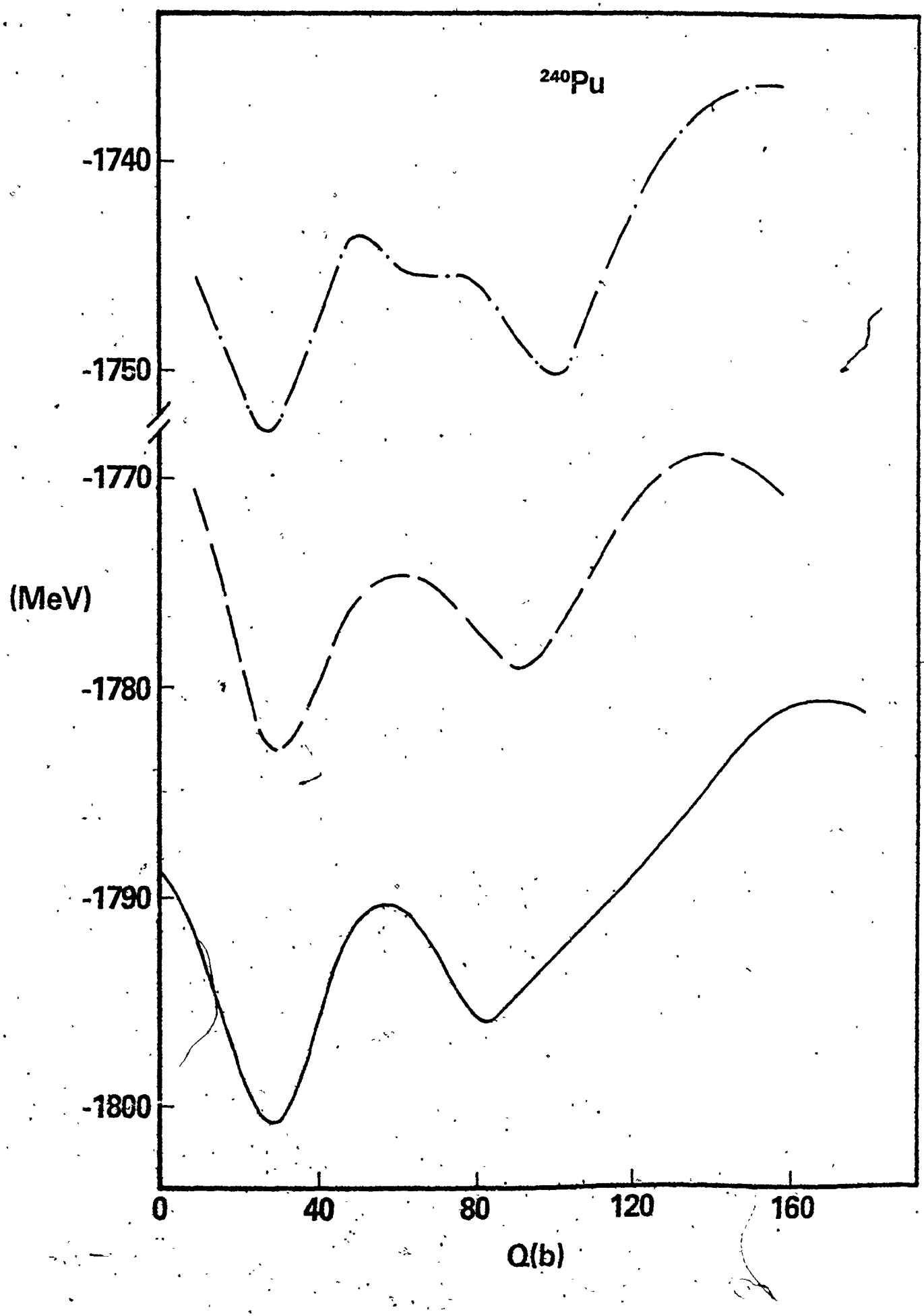
^{240}Pu
-1740
-1750
-1770
-1780
-1790
-1800
(MeV)
0
40
80
120
160
Q(b)

occurs at a smaller value of the quadrupole moment, and is too low by about 6 MeV. If we take in our calculation $N_{cut} = 16$ rather than 18, our curve does not change for smaller deformations but the agreement with the CHF curve near the second barrier is much more improved. We have also repeated the calculations with a quadratic constraint for a few points near the second barrier with $N_{cut} = 18$. The resulting barrier height was found to be within an MeV of the result with the linear constraint. We also tested our method starting with more sophisticated potentials of the type proposed by Brack[27]. From a spherical self-consistent field for ^{208}Pb, depth of the neutron and proton Woods-Saxon fields were approximately fitted and the half-fall-off radius was fitted with a $A^{1/3}$ dependence. Also, the effective mass was parametrized according to Brack's prescription. Calculations in our approximation with this field showed that the disagreement with the CHF result near the second barrier persisted. It should be mentioned here that the centre-of-mass correction has not been included in our calculation. The CHF curve includes the correction in the one-body approximation which is about 20 MeV. This is close to the difference in absolute energies between the CHF and the TSIM curves. We have also plotted the zeroth order energy $E^{(0)}$ which is much worse. One can note that although the position of the second minimum in $E^{(0)}$ is way off the CHF estimate, the corrections after one iteration do try to shift the position of the minimum in the right direc-

tion.

IV.4 Corrections

As such our calculation of the fission barrier cannot be directly compared with experimental value, since both our estimate and the CHF calculation have been made under many simplifying conditions. The best one can do then is to make a rough estimate of the contributions due to the factors neglected in the calculations.

In the fission process the total angular momentum is conserved. However the HF calculations yield an intrinsic state of the system which is an admixture of states of the ground state rotational band. In the spherical limit, the nucleon states can couple to form different J-states which are degenerate in the single particle limit. Even when the two-body interaction is introduced, these states with different J are separated by small amounts (100-200 keV)[42] and hence can be taken to be degenerate. When the spherical symmetry is broken, this degeneracy breaks down and the HF Slater determinant is no longer an eigenstate of the total angular momentum. Thus, the HF calculation produces a lack in binding energy when the system is deformed. In theory, projection procedures can be used to obtain the energy contribution of the angular momentum component that one is interested in. This can become very cumbersome for heavy nuclei. Instead, one often makes the approximate estimate ΔE_{rot} of the spurious rotational energy by

$$\Delta E_{rot} = \hbar^2 \langle \tilde{J}^2 \rangle / 2\mathcal{J} ,$$

where the expectation value of $\tilde{J}^2$ is taken in the intrinsic state and $\mathcal{J}$ is the moment of inertia which is generally calculated within the Inglis cranking model. For heavy nuclei, ΔE_{rot} can be about $3 \sim 6$ MeV in the ground state and it increases with increasing deformation[28,43]. Relative to the ground state, this correction is about 1 MeV near the first barrier and near the second minimum, and $2 \sim 3$ MeV near the second barrier.

Some hints of other corrections to the CHF calculations are obtained from experiments. The experimental fact that nuclear fission is mass asymmetric in general gives a hint that calculations with shapes not symmetric under the reflection at a plane perpendicular to the fission axis are necessary. Further, axial asymmetry must also be included to see if the barriers are stable against γ-deformations. Some phenomenological calculations suggest[44] that the inner barrier is lowered by about 1 MeV due to the inclusion of γ-degrees of freedom. This correction is in the right direction since the CHF overestimates both barrier heights[13]. The discrepancy between the CHF results and the experimental values cannot be removed by fitting the liquid-drop parameters, since it is well known that the barrier heights are mainly determined by the shell corrections. The liquid-drop energy only accounts for one-third or less of the total fission

thresholds. Besides, the liquid-drop model favours reflection symmetric shapes. Strutinsky-type calculations have been performed[45] with left-right asymmetry. Pauli et al.[46] have used the parametrization of the nuclear shapes given by eqn. (3.8) with $\alpha \neq 0$. The energy is minimized with respect to α in all points of the (c-h) plane. It is found that the region from the ground state to the second minimum is stable against reflection asymmetry for all actinides. Shapes beyond this region are unstable against such deformations. The outer saddle point energy for ^{240}Pu is lowered by about 3 MeV. Also, the position of the second barrier shifts towards a deformation with thinner neck and smaller elongation. This increases the Coulomb repulsion and hence the fragments have higher kinetic energy compared to those in a symmetric fission.

Besides the correction for the various degrees of freedom mentioned above, adjustments have to be made for truncation errors and in the Coulomb exchange energy before any comparison with experiment can be made. All these corrections have been displayed in Table 2[47] along with the experimental numbers. Remembering that the TSIM underestimates the CHF second barrier by about 6 MeV, one finds that the corrected barrier height is about 11-13 MeV which is more than twice the experimental value. The inner barrier is about 8 MeV which is again a little higher compared to the experimental estimates[40,48].

TABLE 2

ERROR ESTIMATES IN CHF CALCULATIONS FOR ^{240}Pu

Corrections	E_A (MeV)	E_B (MeV)
Spurious rotational energy	-1	-2 to -3
Coulomb exchange energy	<+0.5	+0.5 to +1
Truncation error	<-0.5	-2
γ- and mass asymmetry	-1	-4 to -5
Experimental barriers		
Bjørnholm and Lynn	6.0±0.2	5.4 ±0.2
Britt et al.[40]	6.0±0.3	5.35±0.2

Error estimates in CHF calculations of fission barrier of ^{240}Pu. E_A and E_B correspond respectively to the height of the first and the second barrier relative to the ground state minimum. This table is due to Brack[47]. The experimental barrier heights are taken from ref. (13).

IV.5 Comparison of Skyrme-type interactions

To date only the Skyrme-III and Skyrme-IV interactions have been used in CHF calculations for the fission barrier of ^{240}Pu. Flocard[12] in his thesis has shown that even after making the necessary corrections mentioned in sec. IV.4, the outer barrier height is much larger than the experimental value for both these interactions. In these CHF calculations, pairing gap was taken to be a constant. As mentioned in sec. IV.3, the CHF calculation[13] with a surface-dependent G is found to fit the experimental results rather well. This does not necessarily mean that such a choice should be preferred over the choice of constant gap. The question may possibly be settled within the framework of HFB approximation. Gogny[26] has performed HFB calculation with finite range D1 forces for ^{152}Sm. A linear constraint was used to draw energy versus deformation curve. Comparison was made with HF+BCS calculations with two different choices of pairing; a constant Δ and a G proportional to surface. It was found that at large deformations, the prescription of constant Δ is comparatively in better agreement with the HFB results. Some recent HFB calculations[25] also point to the same conclusion.

If then, one accepts that HF+BCS calculations should be carried out with constant gap, it is evident that the Vautherin-Brink version of Skyrme force is not suitable for fission barrier estimates. Indeed, one can find several sets

of parameters for these forces, each set being capable of producing equally good fits to the ground state properties of nuclei. It is therefore necessary that some other criteria be sought for which would bring out the differences in these Skyrme-like forces. One of the properties that can be evaluated in a nuclear matter calculation is the imcompressibility K defined by

$$K = k_F^2 \left(\frac{\partial^2 (\frac{E}{A})}{\partial k_F^2}\right),$$

where k_F is the Fermi momentum at the saturation density and E/A is the energy per nucleon. For the usual Skyrme force, K in nuclear matter is given by[19]

$$K = -15 \frac{E}{A} + \frac{9}{5} \frac{h^2}{2m} k_F^2 + \frac{t_3}{12\pi^4} k_F^6 .$$

Since E/A is about -16 MeV in nuclear matter and k_F around 1.3 fm^{-1}, any Skyrme interaction with a positive value of t_3 will yield a value of K larger than 300 MeV. Blaizot et al.[49] have performed RPA calculations on giant monopole resonances and have estimated the value of K = 210 ± 30 MeV which is much less than that obtained by Skyrme interaction.

Zamick[50] has shown, using harmonic oscillator wave functions, that for a three parameter interaction of the type

$$- A\delta(\underset{\sim}{r}) + B\rho^{\beta}(\underset{\sim}{R})\delta(\underset{\sim}{r}) ,$$

the incompressibility K is linear in the exponent β, and hence

increases with increasing β. In the Vautherin-Brink type Skyrme force β = 1 in the repulsive three-body term in eqn. (2.9) which yields K = 356 MeV for Skyrme III. Moskowski's modified delta interaction[4] has β = 2/3 which gives a lower value of K = 306 MeV. In the Skyrme-type forces with β = 1, K can be lowered to some extent through[51]

$$\frac{h^2}{2m^*} = \frac{h^2}{2m} + \frac{1}{k_F^2}\left\{-15\,\frac{E}{A} - \frac{5}{6}K + \frac{h^2}{m}k_F^2\right\},$$

although very unrealistic values of the effective mass m* will be required to bring down K to a reasonable value. Such values of m* will not yield good single particle spectra. Skyrme-V is just such an example where m*/m = 0.38 which is very small and K = 306 MeV. Thus, it is obvious that while preserving reasonable values of E/A, k_F and m*, the incompressibility can be lowered only through the exponent of the density dependent term in the effective interaction. Similar conclusions were arrived at by Sprung and Banerjee[52] who constructed three effective interactions, namely G0, G1 and G2 interactions from Reid potential with β = 1/6, 1/3 and 1 respectively and the corresponding values of K being 180, 210 and 300 MeV in nuclear matter.

Several attempts have been made to construct Skyrme-type interactions with β < 1 to lower the value of K. Since a survey of the dependence of barrier heights on β may be interesting, we have chosen five Skyrme-type interactions for our study of ^{240}Pu. Most of the fission barrier calculations

being of the Strutinsky-type, it is highly desirable to calculate the energy surface microscopically. While such a project is too expensive in a CHF approximation, our method allows us to do this rapidly. The parameters of the five interactions are displayed in Table 3. The general form of Skyrme-type interaction has been discussed in sec. II.2. Skyrme III (S-III) used earlier for ^{240}Pu has $\beta = 1$. The interaction (SKa) by Köhler[53] has $\beta = 1/3$ which gives K = 263 MeV. A smaller value of $\beta = 1/6$ suggested by the success of G0 force, has been adopted by the Orsay group[54] to construct the interaction SKM with K = 217 MeV. The same value of β has been used by the Kyoto group[55] whose interaction S-MK yields K = 220 MeV. The parameters for the S-MK that are tabulated are preliminary and are slightly different from those in ref. 55. It should be noted that the values of K from SKM and S-MK are close to that suggested from the isoscalar monopole excitations. In fixing the parameters of S-MK the contributions to the charge radius from the neutron form factor and the spin-orbit interaction has been taken into account. Bertozzi et al.[56] have shown that modifications in the proton distribution due to the non-zero charge density in neutrons are important in explaining the electron-nucleus elastic scattering data. Since the ground state properties of spherical nuclei as predicted by S-III, S-V, SKa and SKM are found in the literature, we tabulate the estimates of E/A

TABLE 3

PARAMETERS OF SKYRME-TYPE INTERACTIONS

	t_0 (MeV.fm^3)	x_0	t_1 (MeV.fm^5)	x_1	t_2 (MeV.fm^5)	x_2	t_3 (MeV.fm^6)	x_3	W (MeV.fm^5)	β
S-III	-1128.75	0.45	395.5	0.0	-95.0	0.0	14000.0	1.0	120.0	1
S-V	-1248.29	-0.17	970.56	0.0	107.22	0.0	0.0	-	150.0	-
SKa	-1602.78	-0.02	570.88	0.0	-67.70	0.0	8000.0	-0.286	125.0	1/3
S-MK	-2584.0	0.48	429.0	0.055	-118.2	0.0	14904.0	0.60	125.0	1/6
SKM	-2645.0	0.09	385.0	0.0	-120.0	0.0	15595.0	0.0	120.0	1/6

The form of parametrization is given in the text. (see sec. II.2, eqn. (2.9)). The values of x_3 and β for S-V are undefined since $t_3 = 0.0$.

and root-mean-square charge radius $\sqrt{\langle r_c^2 \rangle}$ obtained from S-MK in Table 4. The parenthesized numbers are the contributions from the Bertozzi correction mentioned above. The estimates are as good as those from other interactions.

For Skyrme-type interaction the effective mass m* is given by

$$\frac{m^*(\underset{\sim}{r})}{m} = \left[1 + \frac{2m}{\hbar^2}(3t_1+5t_2)\rho(\underset{\sim}{r})\right]^{-1},$$

where we have assumed the simplest case of $\rho_n = \rho_p = \frac{1}{2}\rho$. The ratio m*/m is 1 outside the nucleus and has a nearly constant value in the interior. The density in the central region of the nucleus approaches the nuclear matter density, so that the corresponding effective masses are comparable. The nuclear matter values for m*/m are displayed in Table 5. Since the level density is governed by the effective mass, one can choose from various interactions, the one which generates single particle level density close to those obtained from experiments. In a finite nucleus, the level density near the Fermi surface is reasonably well produced if $m^*/m \approx 1$. However, for deeply bound states a smaller value of $m^*/m \approx 0.5$ is required. Beiner et al.[19] have found that a value of $m^*/m \approx 0.75$ is able to achieve an overall reasonable agreement with the experimental data. This is one reason that S-III has been widely preferred over other Skyrme interactions.

TABLE 4

BULK PROPERTIES OF SOME CLOSED NUCLEI WITH THE S-MK INTERACTION

		^{16}O	^{40}Ca	^{48}Ca	^{90}Zr	^{208}Pb
E/A (MeV)	cal.	-128.50	-341.84	-419.34	-781.63	-1637.25
	exp.	-127.62	-342.06	-416.01	-783.62	-1636.49
$\sqrt{\langle r_c^2 \rangle}$ (fm)	cal.	2.73	3.48	3.49	4.27	5.50
		(-0.02)	(-0.02)	(-0.04)	(-0.03)	(-0.02)
	exp.	2.73	3.49	3.48	4.27	5.50

The calculated charge radius $\sqrt{\langle r_c^2 \rangle}$ which includes contributions from the neutron distribution and the spin-orbit interaction which are shown in parentheses for each nucleus, in addition to the standard proton finite size and centre of mass motion correction. The experimental numbers are taken from ref. (19).

From Table 5 one can see that the nuclear matter m*/m for the various interactions are not too different from each other, the only exception being S-V which has a value of 0.38. Such a low value in S-V is due to the fact that the saturation is brought about not due to the density dependence (since $t_3 = 0$) but due to the strong momentum dependence in the effective two-body potential. The ratio m*/m has been shown[19] to increase with increasing t_3.

Another quantity that can be extracted out from nuclear matter is the symmetry energy ε_1. If the nuclear matter contains unequal number of neutrons and protons, then the energy per nucleon can be expanded in powers of the symmetry coefficient $\alpha_s = (N-Z)/A$ as

$$\frac{E(\alpha_s)}{A} = \frac{E(0)}{A} + \varepsilon_1 \alpha_s^2 + \varepsilon_2 \alpha_s^4 + \cdots ,$$

where E/A in Table 5 is E(0)/A and is close to -16 MeV for all interactions. Estimates of the asymmetry energy coefficient ε_1 are displayed in the same table. On comparing with the corresponding estimate of 27.5 MeV from the mass formula fittings[57], one finds that the S-III and S-MK have reasonable symmetry energy..

So far we have compared the nuclear matter properties obtained from these interactions. Besides, for finite nuclei one can also define surface energy which could be important in the study of fission and hence its influence on the defor-

TABLE 5

NUCLEAR MATTER PROPERTIES OF SKYRME-TYPE INTERACTIONS

	k_F (fm^{-1})	E/A (MeV)	m/m*	K (MeV)	ε_1 (MeV)
S-III	1.29	-15.9	0.76	356	28.2
S-V	1.32	-16.1	0.38	306	32.8
SKa	1.32	-16.0	0.61	263	32.9
S-MK	1.33	-15.7	0.75	220	26.6
SKM	1.33	-15.8	0.79	217	30.8

mation energy is worth investigating. The relation between surface energy and the interaction parameters is not simple. However, in order to get a rough idea about the contribution of surface energy to the energy of a nucleus due to various interactions, we fit the liquid-drop (LD) mass formula to the energies of five closed shell nuclei ^{16}O, ^{40}Ca, ^{48}Ca, ^{90}Zr and ^{208}Pb. The Coulomb energy is subtracted prior to the fitting, although the Coulomb interaction in the HF equations is retained so as to obtain reasonable densities. This can be important in heavy nuclei where the Coulomb energy can be as high as one-third of the total energy. The expression chosen for the LD parametrization[17] is

$$E(N,Z) = a_v(1+k_vI^2)A + a_s(1+k_sI^2)A^{2/3} + a_c(1+k_cI^2)A^{1/3} + a_0 , \qquad (4.1)$$

where $I = (N-Z)/A$. The parameters a_v and a_vk_v are the volume energy and volume asymmetry energy coefficients. Likewise, the terms with subscripts s and c refer to the surface and curvature corrections. The role of the last term a_0 is merely to stabilize the other coefficients[58]. The values of a_v and a_vk_v have been set to be those of nuclear matter, since from Table 5, $a_v = E/A$ and $a_vk_v = \epsilon_1$. The remaining five parameters a_s, a_c, k_s, k_c and a_0 are determined uniquely from the energies of the five above mentioned nuclei. These have been listed in Table 6. In the last column, the effective surface

TABLE 6

LIQUID-DROP PARAMETERS FOR SKYRME-TYPE INTERACTIONS

	a_v	$a_v k_v$	a_s	$a_s k_s$	a_c	$a_c k_c$	a_o	a_s'
S-III	-15.9	28.2	17.6	-31.5	15.8	-40.6	-39.8	16.1
S-V	-16.1	32.8	20.7	-107.1	1.2	176.6	-21.0	15.7
SKa	-16.0	32.9	19.1	-88.2	9.2	115.1	-29.8	14.9
S-MK	-15.7	26.6	16.1	-29.1	20.8	-43.4	-45.7	14.8
SKM	-15.8	30.8	15.9	-51.6	19.9	-10.3	-44.2	13.5

The parameters are defined in text (see sec. IV.5, eqn. (4.1)). a_s' in the last column is the effective surface energy for ^{240}Pu, where $a_s' = a_s(1+k_s I^2)$ with $I = (N-Z)/A = 52/240$.

energy $a_s' = a_s(1+k_s I^2)$ for ^{240}Pu is tabulated.

IV.6 Fission barrier of ^{240}Pu revisited

We employ the five forces to trace the deformation energy versus $\langle Q \rangle$ curve of ^{240}Pu using the TSIM. In sec. IV.3 it was shown that the method was reliable up the outer saddle at which it underestimated the second barrier height by about 6 MeV if $N_{cut} = 18$. Although the agreement with the CHF result improved for $N_{cut} = 16$, we have done our calculation with the former choice. Since this underestimation is expected not to depend on the particular interaction used, one can extract some quantitative conclusions from the TSIM calculations.

We plot the deformation energy curves in Fig. 7. The curves corresponding to S-V and SKa are in Fig. 7a and those for SKM and S-MK are in Fig. 7b. S-III result has been plotted in both the figures as a reference curve, since this interaction has been mostly used in the CHF calculations for ^{240}Pu. The first minimum is drawn at zero energy. It should be noted that S-V and SKM yield a slightly lower second minimum compared to the first. In order to compare with the experimental barrier heights (see Table 2), corrections due to spurious rotational energy, γ- and mass-asymmetry, truncation of basis etc. must be made in the TSIM results. These have been given some consideration in sec. IV.4. Also since the Coulomb exchange energy has been included in the Slater approximation which tends to overestimate the total energy,

Fig. 7 Calculated deformation energy of ^{240}Pu as a function of the mass quadrupole moment Q using various Skyrme-type interactions. The zero of energy is taken to be at the first minimum.

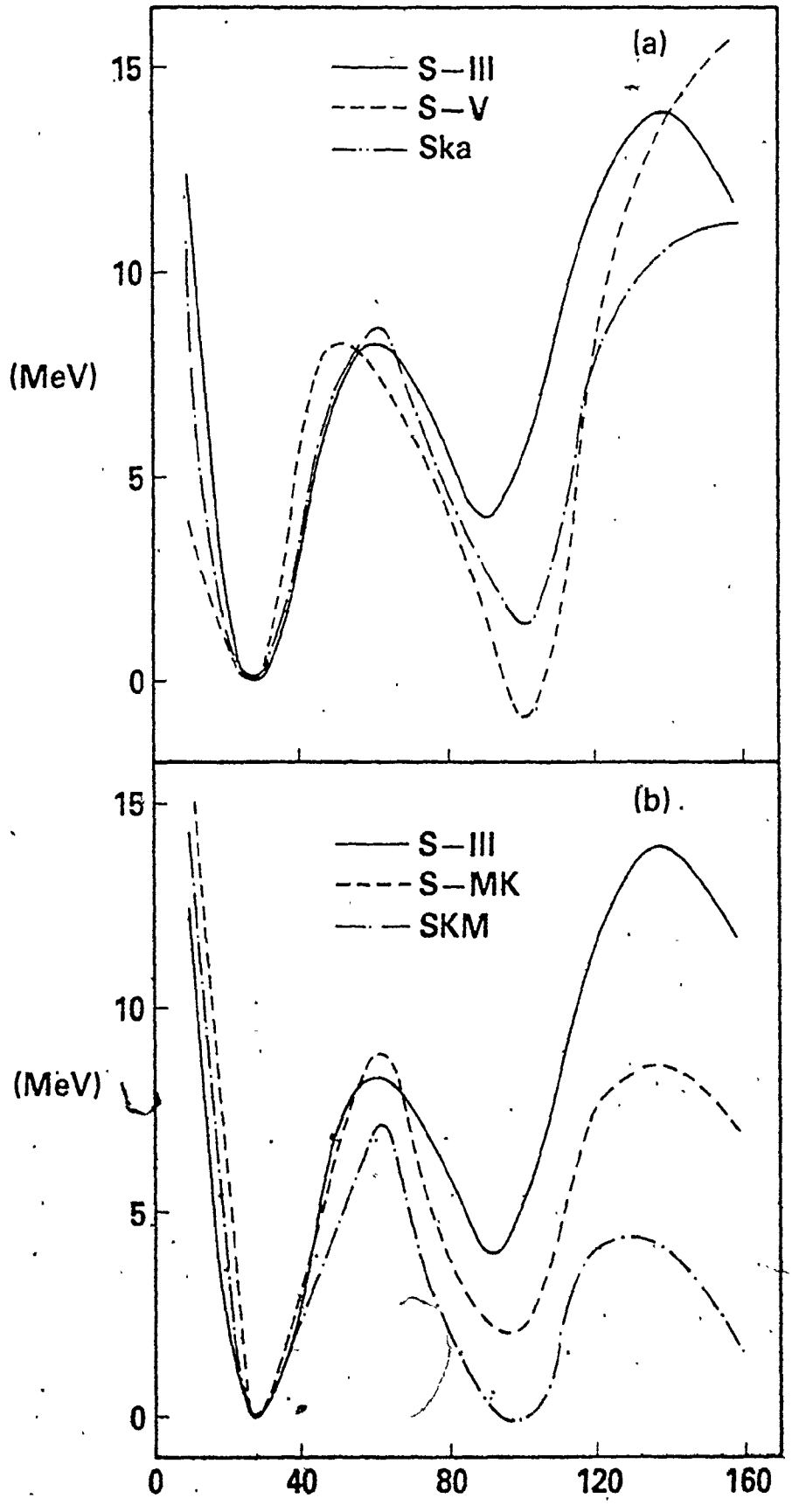
(a)
S—III
S—V
Ska
15
10
5
0
(MeV)
(b)
S—III
S—MK
SKM
15
10
5
0
(MeV)
0
40
80
120
160

adequate correction must be made. All these have been summed up in Table 2 which is due to Brack[47]. The corrected barrier heights are displayed in Table 7. One can see that the estimates from the S-MK interaction are in comparatively better agreement with the experimental values of the barrier heights. It should be pointed out here again that the S-MK yields a value of K which is close to that obtained from isoscalar monopole resonances.

Although the position of first minimum and the first barrier height are nearly the same for all the interactions, large differences are visible near the second saddle. A glance at the values of effective surface energy a_s' for ^{240}Pu in Table 6 shows that an interaction with larger a_s' gives a higher second barrier. However, S-V is an exception. Also, from the same table one can deduce that the barrier height increases with increasing K. Again S-V does not follow this trend. A possible explanation may be due to Flocard[12] who has compared fission barriers of ^{240}Pu obtained from S-III and S-IV. It was found that the latter interaction gives a second barrier height which is about 5-6 MeV larger than that from S-III which too overestimates the experimental height. It can be argued that S-IV has an unrealistic value of the effective mass ($m^*/m = 0.47$), whereas a value close to 0.75 has been shown to be more reasonable[19]. The same may be said about S-V which has $m^*/m = 0.38$. It is well known from the

TABLE 7

HEIGHT OF SECOND BARRIER OF ^{240}Pu WITH SKYRME-TYPE INTERACTIONS

Interaction	E_B' (MeV)	E_B (MeV)
S-III	14.0	11-13
S-V	16.0	13-15
SKa	11.0	8-10
S-MK	8.5	5.5-7.5
SKM	4.5	1.5-3.5

Estimates for the second barrier height by the TSIM. E_B' is the height of the barrier taken from Fig. 7. E_B is the corrected barrier height. The corrections are listed in Table 2 which is 7-9 MeV. A correction of 6 MeV is also necessary because the TSIM underestimates the CHF calculation at the second barrier.

shell-correction approaches that the single particle level densities play an important role in deciding the barrier heights. An interaction with a smaller effective mass produces large spacing between the single particle levels. Consequently, the shell-fluctuations of the deformation energy surface may be large, thereby giving rise to a higher barrier. In addition, the spin-orbit strength parameter W is about 25% larger in S-V than in other interactions. This also enhances shell-fluctuations of the energy surface. In passing, it may be seen from Fig. 7a, that a comparabely small spherical barrier (near $\langle Q \rangle = 0$) for S-V is also a consequence of large W. Barring S-V, all the other four interactions have almost the same effective mass and W. Thus one can expect that the differences in the bulk properties from these interactions may be a crucial factor in producing different barrier heights.

We thus come to the conclusion that Skyrme-type forces with unrealistic values of incompressibility K are not capable of yielding the experimental barrier heights. This does not necessarily mean that a force with a realistic value of K will be able to reproduce the experimental heights. This can be seen from Table 5 where SKM and S-MK have nearly the same values of K, but the resulting barrier heights are very different. At this point, analysis of the surface energy becomes important. Looking at a_s is Table 6 it is clear that

these two interactions contribute quite differently to the surface energy. SKM having a smaller value of a_s' than S-MK gives rise to a lower barrier. It might therefore seem that surface energy coefficients in S-MK are more reasonable than in other forces because it produces the correct barrier heights in ^{240}Pu. Finally, as a result of analysis of ^{240}Pu deformation energy curves, we can say that the procedure of fitting of parameters of Skyrme-type forces only through the ground state properties of nuclei is not good enough and that fission barrier calculations should be taken into consideration for pinning down the force parameters

IV.7 Fission barriers of some actinides

The success of shell correction method has been well recognized in its ability to explain mass-asymmetric fission and the existence of double barriers. Quantitative agreement with experimental results have been obtained for the barrier heights. Further, the observed trend that the inner barrier is lower for actinides lighter than ^{236}U whereas the outer barrier is lower for heavier actinides, is also confirmed in general by the SCM. However, the SCM has not been able to explain the so-called "Th-anomaly". It is of interest to see if a self-consistent calculation is able to remove the anomaly. In sec. IV.7a we examine the barrier heights of ^{232}Th obtained from the TSIM calculation. The SCM calculations have shown that the outer barrier of Fm-

isotopes decreases with increasing neutron number. We have investigated this by looking at the barrier heights of ^{252}Fm and ^{258}Fm in sec. IV.7b. In sec. IV.6 it was shown that the S-MK interaction gave the best agreement with the experimental barrier heights of ^{240}Pu. The same interaction, therefore, has been used in the subsequent calculations.

IV.7a Fission barrier of ^{232}Th

Experimental fission barriers of actinides have been compiled and compared with the SCM calculations by Britt[58] and by Habs et al.[59]. For outer barrier the agremeent between theory and experiment is within 1∿2 MeV for all actinides. The same conclusion is true for inner barrier of nuclides with neutron number $N \geq 140$. However, it is found that theoretical values for inner barriers of nuclides with $N < 140$ are too low. This discrepancy increases, in general, as the neutron number decreases. For the lightest thorium isotopes the difference between theory and experiment is about 4 MeV. This is the well known "Th-anomaly", although the anomaly is not restricted to thorium. Since the uncertainties in the SCM calculations are smaller than 1-2 MeV, it is quite likely that these uncertainties and the errors in determination of liquid drop parameters due to lack of self-consistency may not be enough to explain the anomaly.

Möller and Nix[60] have proposed an interesting explanation for the Th-anomaly. They suggest that the second saddle is split into two individual saddle points separated by a shallow minimum. However, since this anomaly is not restricted to Th-isotopes, a systematic search for third minimimum in all actinides is desired which has not been attempted yet. If such a minimum is found, then one may again have to look carefully at the shell-correction method which has been so successful otherwise.

To see if a self-consistent calculation can throw some light on the Th-anomaly, we have used the TSIM to obtain the deformation energy versus <Q> curve of ^{232}Th, displayed in Fig. 8. The energies are relative to the first minimum. After making the necessary corrections using Table 2, it is found that the outer barrier height is in agreement with the experimental values. The inner barrier height is about 3-4 MeV which compares well with the SCM estimates[59] but is in disagreement with the experimental value of 6 MeV[58,59]. It must be remembered that these calculations are static in nature and whether a dynamical calculation can give any clue to the problem is an open question.

Fig. 8 Deformation energy of ^{232}Th as a function of the mass quadrupole moment Q estimated by the TSIM. The S-MK interaction has been used.

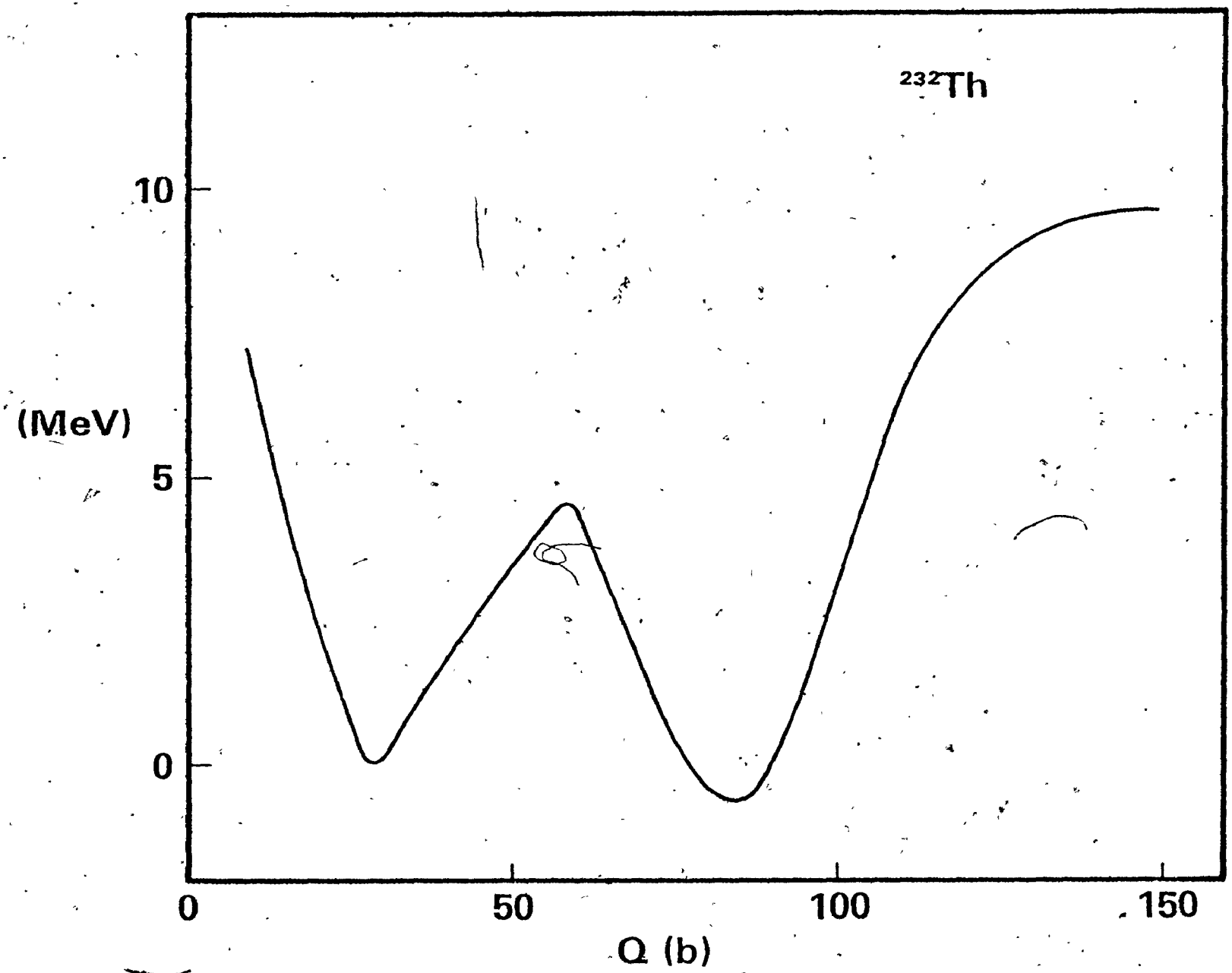
^{232}Th
10
5
0
(MeV)
0
50
100
150
Q (b)

IV.7b Fission barrier of Fm-isotopes

Experiments on the fission of Fm-isotopes have revealed[61] that a transition from mass-asymmetric to mass-symmetric fission occurs between ^{256}Fm and ^{258}Fm. This behaviour has been explained in terms of energetically preferred formation of fragments in the region of doubly magic $^{132}_{50}$Sn nucleus[62]. Shell correction calculations[63] have confirmed the disappearance of outer barrier for ^{258}Fm. As a consequence of the absence of outer barrier, mass-symmetric fission occurs since the inner barrier is stable against asymmetric fission. Further, since the liquid drop prefers symmetric fission and has only one barrier, the absence of second barrier in Fm-isotopes which undergo symmetric fission is understandable.

Two isotopes, ^{252}Fm and ^{258}Fm have been considered here. Fig. 9 exhibits the deformation energy versus quadrupole moment curves. As usual, the zero of energy is taken to be at the position of first minimum. Dark circles in the graph for ^{232}Th correspond to TSIM calculations with the S-III interaction. The resulting second barrier is about 6 MeV higher than the corresponding barrier obtained from the S-MK interaction. This is in agreement with the trend followed in the ^{240}Pu barrier systematics in sec. IV.6. When corrections to the outer barrier are made using Table 2, it is found that ^{258}Fm does not exhibit a second barrier. The correction due to mass-asymmetry

Fig. 9 Calculated deformation energies of ^{252}Fm and ^{258}Fm as a function of the mass quadrupole moment Q using the S-MK interaction. The dots in the upper graph correspond to energies with S-III.

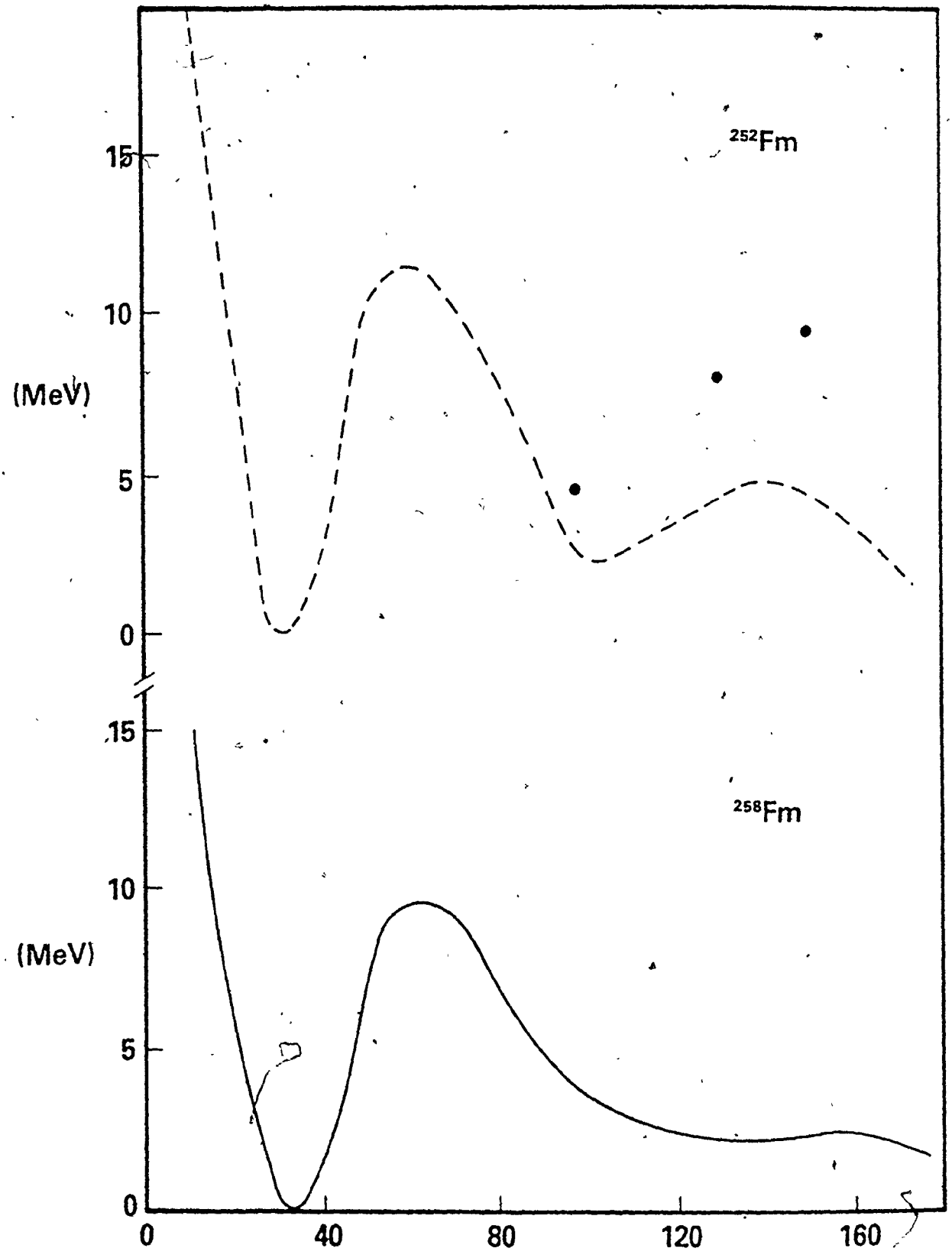
^{252}Fm
15
10
(MeV)
5
0
^{258}Fm
15
10
(MeV)
5
0
0
40
80
120
160

which is about 3 MeV is not included since our TSIM calculation is done for mass-symmetric fission, in accordance with experimental observation for ^{258}Fm. It was not possible to undertake a systematic study of variation of outer barrier height in heavier actinides because of the limitations of storage in computer and therefore the increase in truncation errors.

CONCLUSIONS

A simple but accurate method which is an approximation to the Hartree-Fock technique of self-consistent calculations has been devised. The method (TSIM) which uses only the first two iterations of the self-consistency cycle has been shown to yield binding energies of spherical nuclei close to their corresponding HF estimates. The TSIM has been shown to produce deformation energy curves in close correspondence with those from the CHF technique. The Vautherin-Brink version of Skyrme interaction has been used for all these calculations. The S-III interaction is one of them and has been shown to be incapable of producing the correct fission barrier heights. For such calculations the choice of pairing strength is important. The choice of constant gap, which is shown to be reasonable by HFB calculations[26] has been chosen for the fission barrier estimates. Five Skyrme type interactions have been employed for fission barrier calculation of ^{240}Pu. They show a systematic variation of the second barrier height with incompressibility K and the effective surface energy a_s'. Higher values of K and a_s' give higher barriers. This trend is somewhat disturbed by S-V which is ascribed to its very small unrealistic effective mass. The S-MK interaction is found to give most reasonable agreement with the experimental barrier height for ^{240}Pu.

Calculations of deformation energies for some other actinides, performed with S-MK bring out some interesting results. The results for ^{232}Th indicate that Hartree-Fock calculations with Skyrme-type forces may not be able to explain the Th-anomaly. The deformation energy curve for ^{258}Fm shows no second barrier, in agreement with experiment.

Our TSIM calculations, as well as the present day CHF calculations have many limitations which have been taken care of in an approximate manner in Table 2. Although our (and HF) calculations lack in dynamical treatment of the system, the success of the adiabatic approach of shell-correction method hints that it is still meaningful to carry out a microscopic calculation in the adiabatic limit. Thus, from our calculation of fission barriers it is evident that in order to choose between various effective forces, a survey of their ground state properties of nuclei is not enough but that fission barrier calculations must also be taken into account.

REFERENCES

1. A. K. Kerman, J. P. Svenne and F.M.H. Villars, Phys. Rev. 147 (1966) 710.
2. K. A. Brueckner, J. L. Gammel and H. Weitzner, Phys. Rev. 110 (1958) 431.
   J. Nemeth and D. Vautherin, Phys. Lett. 32B (1970) 561.
3. H. A. Bethe, Ann. Rev. Nucl. Sci. 21 (1971) 93.
4. S. A. Moszkowski, Phys. Rev. C2 (1970) 402.
5. T.H.R. Skyrme, Phil. Mag. 1 (1956) 1043.
6. D. Vautherin and D.M. Brink, Phys. Rev. C5 (1972) 626.
7. D. Vautherin, Phys. Rev. C7 (1973) 296.
8. H. Flocard, P. Quentin and D. Vautherin, Phys. Lett. 46B (1973) 304.
   M. Caillau, J. Letessier, H. Flocard and P. Quentin, Phys. Lett. 46B (1973) 11.
9. H. Flocard, P. Quentin, A. K. Kerman and D. Vautherin, Nucl. Phys. A203 (1973) 433.
10. J. W. Negele and D. Vautherin, Phys. Rev. C5 (1972) 1472.
11. D. Kolb, R. Y. Cusson and H. W. Schmitt, Phys. Rev. C10 (1974) 1529.
12. H. Flocard, Thése d'Etat, Orsay (1975).

13. H. Flocard, P. Quentin, D. Vautherin, M. Véneroni and A. K. Kerman, Nucl. Phys. A231 (1974) 176.

14. V. M. Strutinsky, Nucl. Phys. A95 (1967) 420; A122 (1968) 1.

15. S. G. Nilsson, C. F. Tsang, A. Sobiczewski, Z. Szymanski, S. Wycech, C. Gustafson, I. Lamm, P. Möller and B. Nilsson, Nucl. Phys. A131 (1969) 1.

16. O. Bohigas, X. Campi, H. Krivine and J. Treiner, Phys. Lett. 64B (1976) 381.

17. Y. H. Chu, B. K. Jennings and M. Brack, Phys. Lett. 68B (1977) 407.

18. I. Easson , M. Vallières and R. K. Bhaduri, Phys. Rev. C19 (1979) 1089.

19. M. Beiner, H. Flocard, N. V. Giai and P. Quentin, Nucl. Phys. A238 (1975) 29.

20. H. Flocard, M. Beiner, P. Quentin and D. Vautherin, Proc. Int. Conf. on Nuclear Physics, Vol. 1, Munich, 1973 (North-Holland, Amsterdam, 1974) p. 40.

21. X. Campi and D. W. L. Sprung, Nucl. Phys. A194 (1972) 401.

22. M. Brack, J. Damgaard, A. S. Jensen, H. C. Pauli, V. M. Strutinsky and C. Y. Wong, Rev. Mod. Phys. 44 (1972) 320.

23. J. Damgaard, H. C. Pauli, V. V. Pashkevich and V. M. Strutinsky, Nucl. Phys. A135 (1969) 432.

24. H. C. Pauli, Phys. Rep. 7C (1973) 35.

25. J. F. Berger and M. Girod, Proc. 4th IAEA Symp. Physics and Chemistry of Fission, Jülich 1979, paper IAEA-SM/241-C2, to be published by IAEA (Vienna).

26. D. Gogny, Nuclear self-consistent fields, ICTP Conf. Trieste, 1975, ed. G. Ripka and M. Porneuf (North-Holland, Amsterdam, 1975) p. 333.

27. M. Brack, Phys. Lett. 71B (1977) 239.

28. C. M. Ko, H. C. Pauli, M. Brack and G. E. Brown, Nucl. Phys. A236 (1974) 269.

29. O. Hahn and F. Strassmann, Naturwissenschaften 27 (1939) 11; 27 (1939) 89.

30. N. Bohr and J. A. Wheeler, Phys. Rev. 56 (1939) 426.

31. S. Cohen and W. J. Swiatecki, Ann. Phys. 19 (1962) 67.
S. Cohen and W. J. Swiatecki, Ann. Phys. 22 (1963) 406.

32. P. Möller, Nucl. Phys. A192 (1972) 529.
P. Möller and J. R. Nix, Proc. 3rd IAEA Symp. Physics and Chemistry of Fission, Rochester, N.Y. 1 (1973) 103.

33. V. V. Pashkevich, Nucl. Phys. A169 (1971) 275.

34. M. Brack and P. Quentin, Phys. Lett. 56B (1975) 421.

35. B. K. Jennings and R. K. Bhaduri, Nucl. Phys. A237 (1975) 149.

36. R. A. Schmitt and R. B. Duffield, Phys. Rev. 105 (1957) 1277.

37. J. A. Northrup, R. G. Stokes and K. Boyer, Phys. Rev. 115 (1959) 1277.

38. G. M. Raisbeck and J. W. Cobble, Phys. Rev. 153 (1967) 1270.

39. H. C. Britt, S. C. Burnett, B. H. Erkkila, J. E. Lynn and W. E. Stein, Phys. Rev. C4 (1971) 1444.

40. H. C. Britt, M. Bolsterli, N. J. Nix and J. L. Norton, Phys. Rev. C7 (1973) 801.

41. P. Quentin, Invited Paper to the Sixth International Conference on Atomic Masses, Michigan State University, 1979.

42. I. Kelson, Y. Shoshani, Phys. Lett. 40B (1972) 58.

43. C. K. Ross and C. S. Warke, Phys. Rev. Lett. 30 (1973) 55.

44. V. V. Pashkevich, Nucl. Phys. A133 (1969) 400.
S. E. Larsson, I. Ragnarsson and S. G. Nilsson, Phys. Lett. 38B (1972) 269.
U. Götz, H. C. Pauli and K. Junker, Phys. Lett. 39B (1972) 436.

45. P. Möller and S. G. Nilsson, Phys. Lett. 31B (1970) 283.

46. H. C. Pauli, T. Ledergerber and M. Brack, Phys. Lett. 34B (1971) 264.

47. M. Brack, Proc. 4th IAEA Sym. Physics and Chemistry of Fission, Jülich, 1979, paper IAEA-SM-241/C1, to be published by IAEA (Vienna).

48. H. Weigmann and J. P. Theobald, Nucl. Phys. A187 (1972) 305.

49. J. P. Blaziot, D. Gogny and B. Grammaticos, Nucl. Phys. A265 (1976) 315.

50. L. Zamick, Phys. Lett. 45B (1973) 313.

51. X. Campi, Nuclear self-consistent fields, ICTP Conf. Trieste, 1975, ed. G. Ripka and M. Porneuf (North-Holland, amsterdam, 1975) p. 271.

52. D.W.L. Sprung and P. K. Banerjee, Nucl. Phys. A168 (1971) 273.

53. H. S. Köhler, Nucl. Phys. A258 (1976) 301.

54. H. Krivine, J. Treiner and O. Bohigas, Nucl. Phys. A336 (1980) 155.

55. S. Nishizaki, M. Kohno and K. Ando. Contribution paper in 1980 RCNP International Symposium on Highly excited states in nuclear reactions (Osaka, Japan).

56. W. Bertozzi, J. Friar, J. Heisenberg and J.W. Negele, Phys. Lett. 41B (1972) 408.

57. W. D. Myers and W. J. Swiatecki, Nucl. Phys. 81 (1966) 1. A.G.W. Cameron and R. Elkin, Can. J. Phys. 43 (1965) 1288.

58. H.C. Britt, Proc. 4th IAEA Symp. Physics and Chemistry of Fission, Jülich, 1979, paper IAEA-SM-241/A1, to be published by IAEA (Vienna).

59. D. Habs, H. Klewe-Nebenius, V. Metag, B. Neumann and H. J. Specht, Z. Physik A285 (1978) 53.

60. P. Möller and J. R. Nix, Nucl. Phys. A229 (1974) 269.

61. W. John, E. K. Hulet, R. W. Lougheed and J. J. Wesolowski, Phys. Rev. Lett. 27 (1971) 45.

62. M. G. Mustafa, U. Mosel and H. W. Schmitt, Phys. Rev. C7 (1973) 1519.

63. M. G. Mustafa and R. L. Ferguson, Phys. Rev. C18 (1978) 301.